AFFDL-TR-74-74
Appendix I

# A METHOD FOR PREDICTING ACOUSTICALLY INDUCED VIBRATION IN TRANSPORT AIRCRAFT

TECHNICAL REPORT AFFDL—TR—74—74, APPENDIX I

SEPTEMBER 1974



AIR FORCE FLIGHT DYNAMICS LABORATORY
AIR FORCE SYSTEMS COMMAND
WRIGHT—PATTERSON AIR FORCE BASE, OHIO 45433

## NOTICE

When Government drawings, specifications, or other data are used for any purpose other than in connection with a definitely related Government procurement operation, the United States Government thereby incurs no responsibility nor any obligation whatsoever; and the fact that the government may have formulated, furnished, or in any way supplied the said drawings, specifications, or other data, is not to be regarded by implication or otherwise as in any manner licensing the holder or any other person or corporation, or conveying any rights or permission to manufacture, use, or sell any patented invention that may in any way be related thereto.

Copies of this report should not be returned unless return is required by security considerations, contractual obligations, or notice on a specific document.

AIR FORCE/56780/21 January 1975 — 150

# A METHOD FOR PREDICTING ACOUSTICALLY INDUCED VIBRATION IN TRANSPORT AIRCRAFT

Harold W. Bartel
Cecil W. Schneider

Lockheed-Georgia Company
Marietta, Georgia

## FOREWORD

This report was prepared by the Lockheed-Georgia Company, Marietta, Georgia, for the Aerospace Dynamics Branch, Vehicle Dynamics Division, Air Force Flight Dynamics Laboratory, Wright-Patterson Air Force Base, Ohio, under contract F33615-73-C-3038. The work described herein is a continuing part of the Air Force Systems Command's exploratory development program to obtain accurate and reliable methods of vibration prediction, control, and measurement for flight vehicles.

The work was directed under Project 1370, "Dynamic Problems in Flight Vehicles," and Task 137002, "Flight Vehicle Vibration Control." Captain James E. Marsh (AFFDL/FYS) was the Project Engineer. The Lockheed program manager and principal investigator was Mr. Harold W. Bartel, assisted by Mr. Cecil W. Schneider.

This work is reported in two separate documents. The Lockheed identification of this document is LG74ER0121. The first document is AFFDL-TR-74-74, "Acoustically Induced Vibration in Transport Category Aircraft," and is identified by Lockheed as LG74ER0120. It contains a description of the vibration measurements, tests, analyses, and derivations leading to the method described in this appendix.

Submittal of the technical report by the author in September 1974 completed the contract, which was initiated in February 1973.

This technical report has been reviewed and is approved.

Walter J. Mykytow

WALTER J. MYKYTOW
Asst. for Research & Technology
Vehicle Dynamics Division

## ABSTRACT

A method is set forth for predicting the acoustically induced structural vibration in transport category aircraft. Charts are presented which correlate third-octave random noise and vibration levels at various confidence levels, for the frequency range of 50 to 2500 Hertz. The prediction charts are based on measured data from modern transport aircraft and are presented for the normal direction, ground operation, and a reference structural mass and rigidity. Shell-type structure (fuselage, pods, fairings) and box-type structure (wing, horizontal/vertical stabilizer) are treated separately. Means are provided for predicting lateral and tangential vibration, vibration in pressurized cruise flight, and for correcting for changes in structural mass and rigidity. Application of the method to a hypothetical airplane design case is illustrated in an example.

# TABLE OF CONTENTS

## LIST OF ILLUSTRATIONS

## LIST OF ILLUSTRATIONS - CONTINUED

## LIST OF SYMBOLS, ABBREVIATIONS, AND SUBSCRIPTS

### SYMBOLS

A Cross sectional area - $in^2$

a Dimension of panel bay in the X-direction; rib or stringer spacing - in

b Dimension of panel bay in the Y-direction; beam or frame spacing - in

C Correction factor

D Rigidity - lb - $in^2$

E Modulus of elasticity - $lb/in^2$

h Skin thickness

I Cross sectional area moment of inertia - $in^4$

M Mass - lb/in

X Coordinate direction; panel length

Y Coordinate direction; panel length

$\rho$ Weight density - $lb/in^3$

### SUBSCRIPTS

C Corrected quantity

F Flight quantity

f Frame

L Lateral direction

P Predicted

p Skin plate

R Reference

s Stringer

rms Root-mean-square

### ABBREVIATIONS

dB Decibel (Re: .0002 microbar)

Fus Fuselage

$G_{rms}$ Acceleration in multiples of gravitational acceleration; G = A/g; A is item acceleration in $in/sec^2$; g is 386 in/sec

Hz Hertz; cycles per second

Lat Lateral

Norm Normal

Pred Predicted

Ref Reference

SPL Sound pressure level

Tan Tangential

# INTRODUCTION

Estimates of vibration level are vital to the preliminary design of new aircraft. This requires consideration of all sources of vibration for all representative missions and flight conditions. Because sources, missions, and flight conditions vary widely among different categories of aircraft, it is expedient to tailor vibration prediction methods to specific categories. In transport category aircraft, vibration may be induced by runway roughness, wheel unbalance, atmospheric disturbance, unsteady aerodynamic flow, engine unbalance, auxillary equipment operation, engine noise, boundary layer noise, and other independent causes, each sufficiently different to require separate consideration in the vibration prediction process. At any instant in time, the vibration at any particular point on the structure of a transport aircraft may be the net result of various of these sources in combination. The success of the analyst in predicting the complete vibration environment will, in large part, hinge on the quality of the methods, data, and information he can assemble to account for these various independent sources.

This publication is intended to improve the analyst's chance for success, by adding to his inventory of tools and information, a method for predicting the acoustically induced vibration in transport category aircraft.

Only the essentials for application of the method are presented in this Appendix. The detailed measurements, tests, analyses, and considerations leading to formulation of the method are described separately in AFFDL-TR-74-74 "Acoustically Induced Vibration in Transport Category Aircraft."

## GENERAL INSTRUCTIONS

This vibration prediction method applies to the prediction of structural vibration induced by the impingement of randomly fluctuating sound pressures on the exterior surface, in the frequency range of 50 to 2500 Hertz. The method consists of a series of charts (Figures 1 through 18) which correlate third-octave band noise and vibration levels for a "reference" structure, with corrections (Figures 19 through 22) to account for direction, pressurized flight, mass, and rigidity effects. These charts are based largely on data measured on two contemporary jet transport aircraft, and are presented for the normal direction, ground operation, and a specific reference structural mass and rigidity.

In past formulations the practice has been to establish such charts according to zones of structural similarity. However, a means is included here to account for variations in structural mass and rigidity, which eliminates much of the need for a zonal classification. The charts are limited to two basic structural types: shell structure, and box structure, exemplified by Figure 23. Shell structure is conventional skin-frame-stringer structure, or the equivalent, as used in fuselages, landing gear pods, fairings, etc. Box structure is the skin-stiffened box-beam type structure commonly used in wings, and vertical and horizontal stabilizers.

For each type of structure there is a set of noise-vibration correlation charts; one for each third-octave band. Each chart contains four confidence level lines; 50%, 80%, 90% and 97.5%. These confidence levels are the confidence, or percent probability, that any particular vibration measurement will fall on or below the line. Thus, for the 80% confidence line, there is 80% chance that a particular measurement would be below the line, and 20% chance that it would be above the line. The 50% confidence line is the mean or regression line.

Vibration levels are specified in terms of third-octave root-mean-square accelerations - $G_{rms}$. These are the structural responses to randomly fluctuating third-octave sound pressures in decibels. The charts are not valid for discrete frequency or periodic sound pressures (e.g. propeller noise, gunfire, pure tone acoustical resonance in a cavity, etc.).

The noise-vibration charts are for the reference condition of vibratory motion in a direction normal to the surface of the structure. Correction charts (Figures 19 and 20) are included for obtaining $G_{rms}$ in the lateral and tangential directions. The normal, lateral, and tangential

directions are defined in relation to the structural element, such as a frame, stringer, or wing beam. They have no fixed relation to the major axes of the airframe, or the earth. Normal always means perpendicular to the external surface; lateral means parallel to the surface and perpendicular to the lengthwise direction of the structural element; tangential means parallel to the surface and in the lengthwise direction of the element. For a further definition of vibratory direction, see Figure 24.

## Information Required

A knowledge of the new airplane mission, the purpose of the vibration prediction, and the amount of prediction refinement work to follow, are necessary when considering confidence level, vibratory direction, and operating conditions. Beyond this, the following specific information is necessary to use this method:

Sound pressure level: third-octave band sound pressure levels at the surface of the structure for the airplane operating conditions for which vibration predictions are to be made.

Confidence level: a definition of the confidence level at which the prediction is to be made. Confidence level should take into account the "quality" of the noise levels; the planned use for the predictions (equipment fatigue, equipment malfunction or error, structural analysis, etc.) and the degree of risk acceptable and consistent with cost, weight, and airplane mission. If the vibration prediction is to be used for analysis or test of a component whose failure would cause loss of the aircraft, a confidence level of 95% or greater is suggested. Lesser confidence levels are called for when assessing non safety-of-flight hardware; levels of 80% have been used successfully on some programs.

Structural mass and rigidity: an estimate of the mass and rigidity of the new airplane structure at the point of interest, in units of lbs/in for mass, and lbs - $in^2$ for rigidity. For this method, "mass" is defined as the sum of the weights of all the surface structural components in a 40" by 40" surface area.

For shell type skin-frame-stringer structure, as illustrated in Figure 23

$$M = 40\left[\frac{A_f\rho_f}{b} + \frac{A_s\rho_s}{a} + h\rho_p\right]$$

where M is mass; $A_f$ and $A_s$ are cross-sectional areas in square inches of individual frames and stringers; $\rho_f$, $\rho_s$, and $\rho_p$ are densities of frames, stringers, and skin plate in pounds per cubic inch; h is skin thickness in inches; b is frame spacing in inches; a is stringer spacing in inches; and the constant 40 is the dimension of the structural area in inches.

For box-type beam-rib-plate construction, as illustrated in Figure 23

$$M = 40\left[\frac{A_b\rho_b}{b} + \frac{A_r\rho_r}{a} + \frac{2A_p\rho_p}{40}\right]$$

where $A_b$, $A_r$, and $A_p$ are average individual beam, rib, and plate cross-sectional areas in square inches; $\rho_b$, $\rho_r$, and $\rho_p$ are densities of beams, ribs, and plates in pounds per cubic inch; a is rib spacing in inches; b is beam spacing in inches; the constants 40 are inches; and the constant 2 accounts for an upper and lower plate. Plate cross-sectional area includes risers, in a 40" width.

Rigidity is defined as the sum of the products of modulus and inertia for all of the components in a 40" by 40" surface area. For shell-type skin-frame-stringer structure the skin contribution may be neglected, whereby the rigidity D is

$$D = 40\left[\frac{E_f I_f}{b} + \frac{E_s I_s}{a}\right]$$

where $E_f$ and $E_s$ are moduli of elasticity for frames and stringers in pounds per square inch; $I_f$ and $I_s$ are area moments of inertia for frames and stringers in inches-fourth; a is stringer spacing in inches; b is frame spacing in inches; and the constant 40 is inches.

For box-type beam-rib-plate construction, the rib contribution may be neglected, whereby

$$D = 40\left[\frac{E_b I_b}{b} + \frac{E_p I_p}{40}\right]$$

where $E_b$ and $E_p$ are moduli of elasticity for the beams and plates in pounds per square inch; $I_b$ is area moment of inertia of the beam in inches-fourth; $I_p$ is area moment of inertia for a 40 inch width of the two plates (taken about a neutral axis midway between the plates) in inches-fourth; b is beam spacing in inches; and the constants 40 are inches.

If detailed structural information is lacking but mass can be approximated in some other way, and if it is known that the new airplane structure is of the same general concept as contemporary large jet transport aircraft, then rigidity can be approximated from Figure 25. However, if neither approach is practical, mass and rigidity effects can be neglected pending further structural definition. In this case Figures 1 through 18 are used directly and the predicted levels will be for the mass and rigidity values stated on the figures.

## Specific Instructions

To predict vibration proceed as follows:

### Shell Structure

Obtain rms acceleration from Figures 1 through 9 for the reference case of engine runup on the ground, vibration in the normal direction, structural mass of 0.59 lbs/in, and rigidity of $4.38 \times 10^7$ lbs-in$^2$. These levels may then be modified as appropriate to obtain levels for other mass and rigidity values, other directions, and for pressurized cruise flight. To correct for mass and rigidity effects, compute the mass ratio $M_R/M_P$, and the rigidity ratio $D_P/D_R$, where the subscripts R and P denote values for reference and prediction structure. Enter Figure 21 with the computed mass and rigidity ratios, and obtain the correction factor $C_3$ to be applied to the vibration levels obtained from Figures 1 through 9. The correction factor $C_3$ is valid for all frequency bands.

To obtain vibration level in the lateral or tangential direction, enter Figure 19 or 20 at the same sound pressure level used in Figures 1 through 9, and obtain the level ratio for each frequency band.

To obtain vibration level for pressurized cruise flight, enter Figure 22 at the same confidence level used in Figures 1 through 9 and obtain the level ratio for each frequency band.

Box Structure

Obtain rms acceleration from Figures 10 through 18 for the reference case of engine runup on the ground, vibration in the normal direction, structural mass of 2.24 lbs/in, and rigidity of $1.7 \times 10^{10}$ lbs-in$^2$. These levels may then be modified as appropriate to obtain levels for other mass and rigidity values and other directions. No correction is available for the cruise case (pressurization effects are not applicable.)

To correct for mass and rigidity effects, compute the mass ratio $M_R/M_P$, and the rigidity ratio $D_P/D_R$, where the subscripts R and P denote values for reference and prediction structure. Enter Figure 21 with the computed mass and rigidity ratios, and obtain the correction factor $C_3$ to be applied to the vibration levels obtained from Figures 10 through 18. The correction factor $C_3$ is valid for all frequency bands.

To obtain vibration level in the lateral or tangential direction, enter Figure 19 or 20 at the same sound pressure level used in Figures 10 through 18 and obtain the level ratio for each frequency band.

## ILLUSTRATIVE APPLICATION

The step-by-step procedure for predicting vibration levels using the charts and graphs provided, is exemplified in the following illustrative application. Although the corrections could be combined, and some of the operations omitted, all have been shown independently, and repetitiously, for the sake of clarity.

Consider a hypothetical aircraft modification having the following particulars:

- Long-range subsonic conventional transport intended for electronic surveillance missions.

- Two areas are of interest - one in the fuselage and one in the wing - which will contain equipment. Orientation of the equipment has not been finalized.

- Need preliminary definition of service vibration environment.

- The fuselage surface structure is conventional pressurized skin-frame-stringer aluminum structure. Frames are .080" "Z" sections 4" deep with 1" flanges. Stringers are .090" "Z" sections 2" deep with 3/4" flanges. The frames are spaced at 18"; stringers at 6". The skin is .080".

- The front beam and rib of the outer wing box are in a conventional wet-wall dual-spar aluminum torque box. The front and rear beams are approximately 80" apart. The beams and end ribs are all approximately 0.25" thick "I" sections averaging 16" deep with 3" caps. The internal chordwise ribs are stabilizing trusses spaced at 50". The upper and lower surface plates are 0.14" thick with integral 0.10" thick risers, 2" deep, spaced at 3".

- At the pertinent locations on the surface of the fuselage and the outer wing, noise levels are:

| FREQUENCY BAND Hz | THIRD-OCTAVE BAND NOISE LEVELS - dB | | | |
|---|---|---|---|---|
| | TAKEOFF | | CRUISE | |
| | Fuselage | Wing | Fuselage | Wing |
| 50 | 113 | 124 | 107 | 72 |
| 63 | 115 | 125 | 110 | 75 |
| 80 | 117 | 126 | 114 | 78 |
| 100 | 118 | 128 | 117 | 82 |
| 125 | 119 | 129 | 121 | 86 |
| 160 | 121 | 130 | 123 | 90 |
| 200 | 122 | 132 | 125 | 94 |
| 250 | 123 | 133 | 127 | 98 |
| 315 | 125 | 134 | 125 | 101 |
| 400 | 126 | 135 | 123 | 104 |
| 500 | 128 | 136 | 121 | 108 |
| 630 | 129 | 134 | 118 | 111 |
| 800 | 130 | 132 | 116 | 114 |
| 1000 | 131 | 130 | 114 | 117 |
| 1250 | 129 | 129 | 112 | 119 |
| 1600 | 127 | 128 | 111 | 121 |
| 2000 | 129 | 127 | 110 | 123 |
| 2500 | 133 | 129 | 109 | 125 |

The vibration predictions for this hypothetical case are guided by the following ground rules and observations.

- Vibration should be checked for takeoff vibration conditions. Cruise noise levels are significant in some bands. Vibration will need to be checked under cruise vibration conditions. Therefore, predict vibration for both takeoff and cruise.

- Since equipment orientation is unknown, the definition of the vibration environment should be based on the worst case. Therefore predict vibration for each direction and envelope the spectra.

- The noise levels are an average of measured values for standard day conditions. Occasionally, levels will be higher under certain atmospheric and operational conditions. The structure and equipments must be highly reliable. Some risk of design change is prudent to minimize cost and weight. Therefore predict vibration for the 90% confidence level.

## Fuselage Location

### Takeoff Condition

Figure 1 at 113 dB shows the 50 Hz vibration level at the 90% confidence line to be 0.14 $G_{rms}$. From Figure 1, the 63 Hz level at the 90% confidence line for 115 dB is 0.22 $G_{rms}$. For all bands the levels predicted during takeoff for the reference shell structure in the normal direction, and for the reference mass and rigidity, are tabulated as item 1 in Table I.

The airplane structural mass and rigidity values at the fuselage location are

$$\text{Mass} = M_{Pred} = 40\left[\frac{.080(4+1+1)(.1)}{18} + \frac{.090(2+.75+.75)(.1)}{6} + (.08)(.1)\right] = 0.64 \text{ lb/in.}$$

$$\text{Rigidity} = D_{Pred} = 40\left[\frac{10^7}{18}\left(\frac{.08 \times 4^3}{12} + 2 \times .08 \times 1.96^2\right) + \frac{10^7}{6}\left(\frac{.09 \times 2^3}{12} + 2 \times .75 \times .09 \times .955^2\right)\right]$$

$$= 3.53 \times 10^7 \text{ lbs-in}^2$$

The mass ratio is

$$\frac{M_{Ref}}{M_{Pred}} = \frac{.59}{.64} = 0.92$$

The rigidity ratio is

$$\frac{D_{Pred}}{D_{Ref}} = \frac{3.53 \times 10^7}{4.38 \times 10^7} = 0.81$$

Entering Figure 21 at $M_R/M_P = 0.92$ and at $D_P/D_R = 0.81$ shows the mass and rigidity correction $C_3$ to be 0.90, which is tabulated as item 2 in Table I. Multiplying each of the tabulated $G_{rms}$ reference levels by this correction yields the predicted takeoff vibration level for the fuselage structure, for the normal direction. These values are tabulated as item 3, Table I.

Entering Figure 19, the ratio of lateral-to-normal vibration level, $G_L/G_R$ for the 50 Hertz band and 113 dB is 0.65; for the 63 Hz band and 115 dB, $G_L/G_R$ is 0.77. For all bands, the values of $G_L/G_R$ are tabulated as item 4 in Table I. Multiplying the normal direction levels by these values yields the predicted lateral levels tabulated as item 5, Table I.

Entering Figure 20, the ratios of tangential to normal vibration levels, $G_T/G_R$, are read in like manner, and are tabulated in item 6, Table I. Multiplying the normal direction levels by these values yields the predicted tangential vibration levels, tabulated as item 7, Table I.

Noting the highest of the normal, lateral, and tangential levels, and retabulating the results, yields the predicted takeoff vibration spectrum for the worst direction at the fuselage location, tabulated as item 8, Table I.

Cruise Condition

Using Figure 1, at 107 dB the 50 Hz vibration level for the 90% confidence line is .095 $G_{rms}$. The reference structure vibration levels for all bands are read in like manner and tabulated in item 9 of Table I. The mass and rigidity correction, $C_3 = 0.90$, is tabulated in item 10, Table I. Using Figure 22 to correct the reference levels for pressurized cruise flight, $G_P/G_R$, at 50 Hz and the 90% confidence line, is 0.35. The correction for all bands is read in like manner and tabulated in item 11 of Table I. This correction and the mass-rigidity correction are applied to the item 9 reference levels to obtain the item 12 cruise vibration levels in the normal direction, at the fuselage location.

Entering Figure 19, the ratio of lateral-to-normal vibration level, $G_L/G_R$, for the 50 Hertz band and 107 dB is 0.64. Similarly, ratios are obtained for all bands and are shown in item 13 of Table I. Multiplying the normal direction levels by these values yield the predicted lateral vibration levels, tabulated in item 14, Table I.

Entering Figure 20 the ratio of tangential-to-normal vibration level, $G_T/G_R$, for the 50 Hz band and 107 dB, is 0.62. Similarly, values are obtained for all bands and are shown in item 15 of Table I. Multiplying the normal direction levels by these values yields the predicted tangential vibration levels, tabulated in item 16 of Table I.

Noting the highest of the normal, lateral, and tangential levels and retabulating the results yields the predicted pressurized cruise vibration spectrum for the worst direction at the fuselage location, as tabulated in item 17 of Table I.

The predicted fuselage vibration level in each direction, and the envelope of highest level, for the takeoff and cruise cases, are shown plotted in Figure 26.

## Wing Location

### Takeoff Condition

Entering Figure 10 at 124 dB, the 50 Hz vibration level at 90% confidence is 0.38 $G_{rms}$. From Figure 10 the 63 Hz vibration level at 90% confidence for 125 dB is 0.54 $G_{rms}$. Levels in all bands are obtained in like fashion and tabulated in item 1 of Table II for the reference box structure.

The structural mass and rigidity values at the wing location are

$$\text{Mass} = M_P = 40\left[\frac{.25}{80}(3+3+15.5)(.1) + \frac{2}{40}\left(.14\times 40 + \frac{40}{3}\times 2\times .1\right)(.1)\right] = 1.92 \text{ lbs/in}$$

$$\text{Rigidity} = D_P = 40\left[\frac{10^7}{80}\left(\frac{.25\times 15.5^3}{12} + 2\times .25\times 3\times 7.875^2\right) + \frac{10^7}{40}\left(2\times .14\times 40\times 8.07^2 + 2\times\frac{40}{3}\times .10\times 2\times 7^2\right)\right] = 1.076\times 10^{10} \text{ lbs-in}^2 \text{ (chord-wise trusses neglected)}$$

The mass ratio is $\frac{M_R}{M_P} = \frac{2.24}{1.92} = 1.17$

The rigidity ratio is $\frac{D_P}{D_R} = \frac{1.076 \times 10^{10}}{1.7 \times 10^{10}} = 0.63$

Entering Figure 21 at a mass ratio of 1.17 and a rigidity ratio of 0.63, the mass and rigidity correction is 1.10, as tabulated in item 2 of Table II. Each of the Table II, item 1, reference levels are multiplied by this correction to obtain predicted takeoff vibration levels at the wing location for the normal direction, which are tabulated in item 3 of Table II.

From Figure 19, the ratios of lateral-to-normal vibration level, $G_L/G_R$, at the takeoff noise levels are obtained for each band and tabulated in item 4, Table II. Normal direction levels are multiplied by these ratios to obtain lateral vibration levels, which are tabulated in item 5, Table II.

From Figure 20, the ratios of tangential-to-normal vibration level, $G_T/G_R$, at the wing noise levels are obtained for each band and tabulated in item 6, Table II. Normal direction levels are multiplied by these values to obtain tangential vibration levels, which are tabulated in item 7, Table II.

The highest of the normal, lateral, and tangential levels are noted and retabulated in item 8, Table II to obtain the takeoff vibration spectrum for the worst direction at the outer wing location.

Cruise Condition

Using cruise noise levels, the reference structure vibration levels at 90% confidence are obtained from Figures 10 through 18 and tabulated in item 9 of Table II. Multiplying these levels by the item 10 mass-rigidity correction, the cruise vibration levels in the normal direction are obtained and tabulated in item 11, Table II, for the wing location.

The ratio of lateral-to-normal vibration level, $G_L/G_R$, at the cruise noise levels, are obtained for each frequency band and tabulated in item 12, Table II. Normal direction levels are multiplied by these ratios to obtain the lateral vibration levels tabulated in item 13, Table II.

The ratios of tangential-to-normal vibration level, $G_T/G_R$, at the cruise noise levels, are obtained for each frequency band and tabulated in item 14, Table II. Normal direction levels are multiplied by these ratios to obtain the tangential vibration levels tabulated in item 15, Table II.

The highest of the normal, lateral and tangential vibration levels are noted and retabulated in item 16, Table II to obtain the cruise vibration spectrum for the worst direction at the outer wing location.

The predicted wing beam vibration level in each direction, and the envelope of highest levels, for the takeoff and cruise cases, are shown plotted in Figure 27.

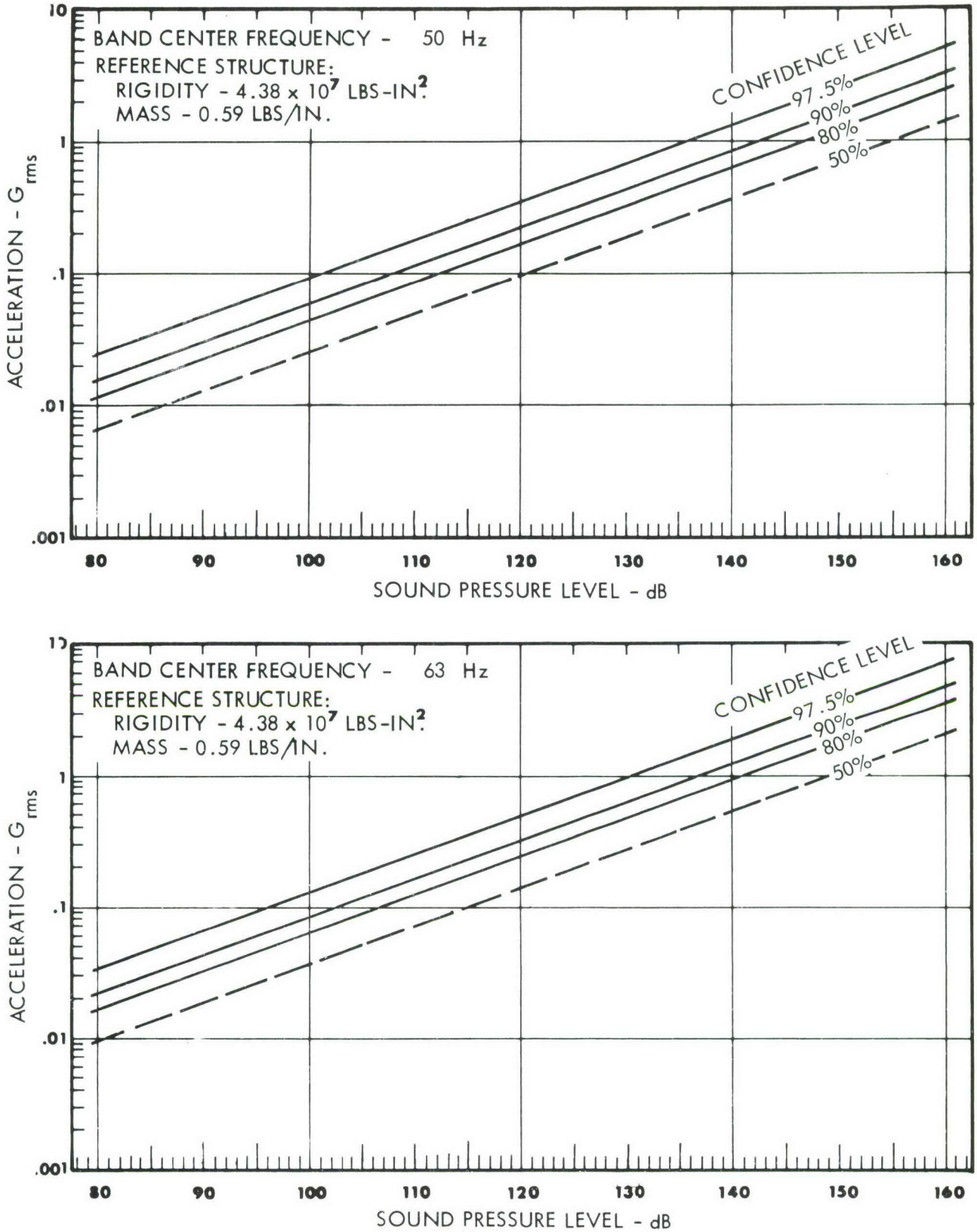


FIGURE 1. THIRD-OCTAVE BAND VIBRATION PREDICTION CHART FOR SHELL STRUCTURE; NORMAL DIRECTION; GROUND OPERATION

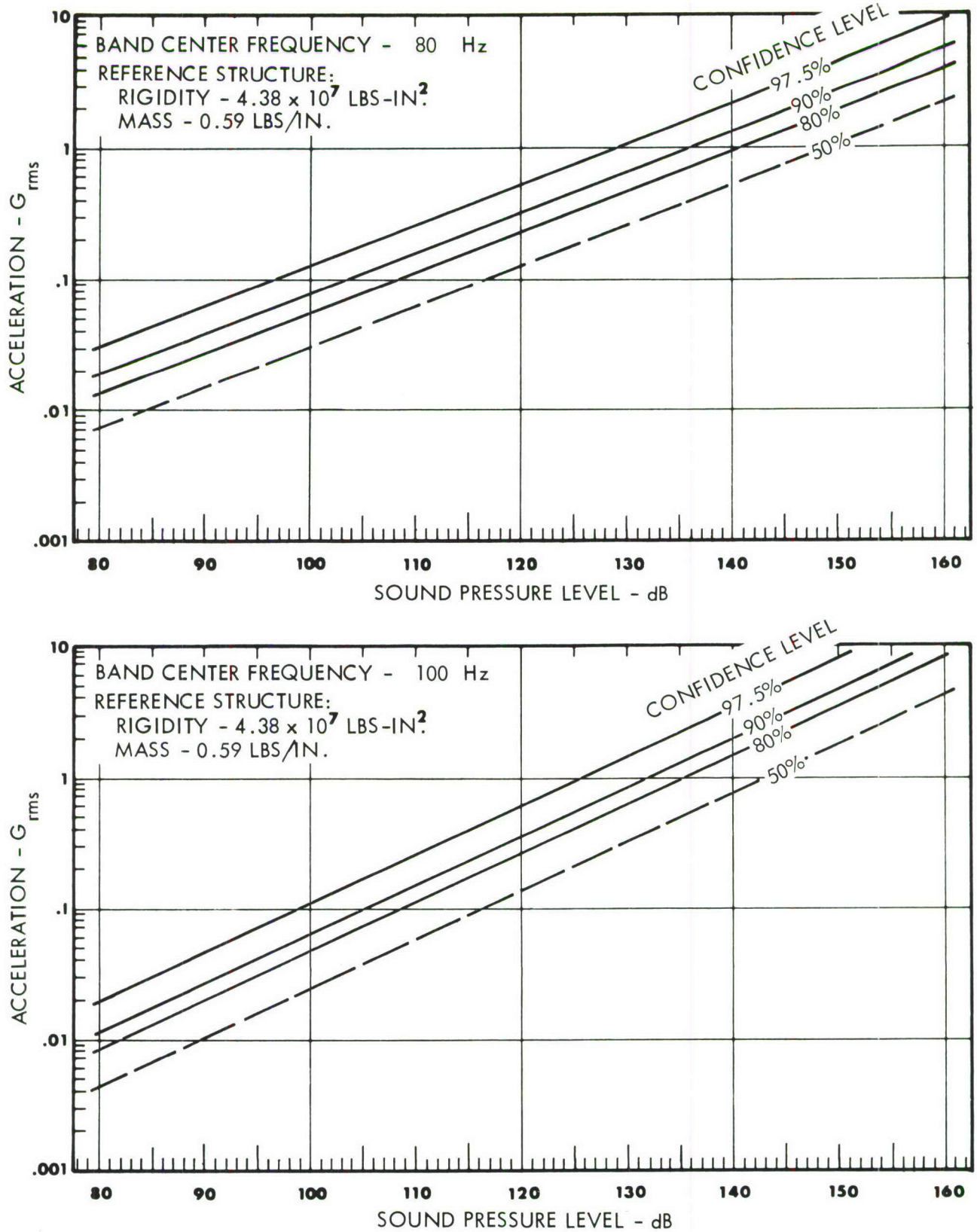


FIGURE 2. THIRD-OCTAVE BAND VIBRATION PREDICTION CHART FOR SHELL STRUCTURE; NORMAL DIRECTION; GROUND OPERATION

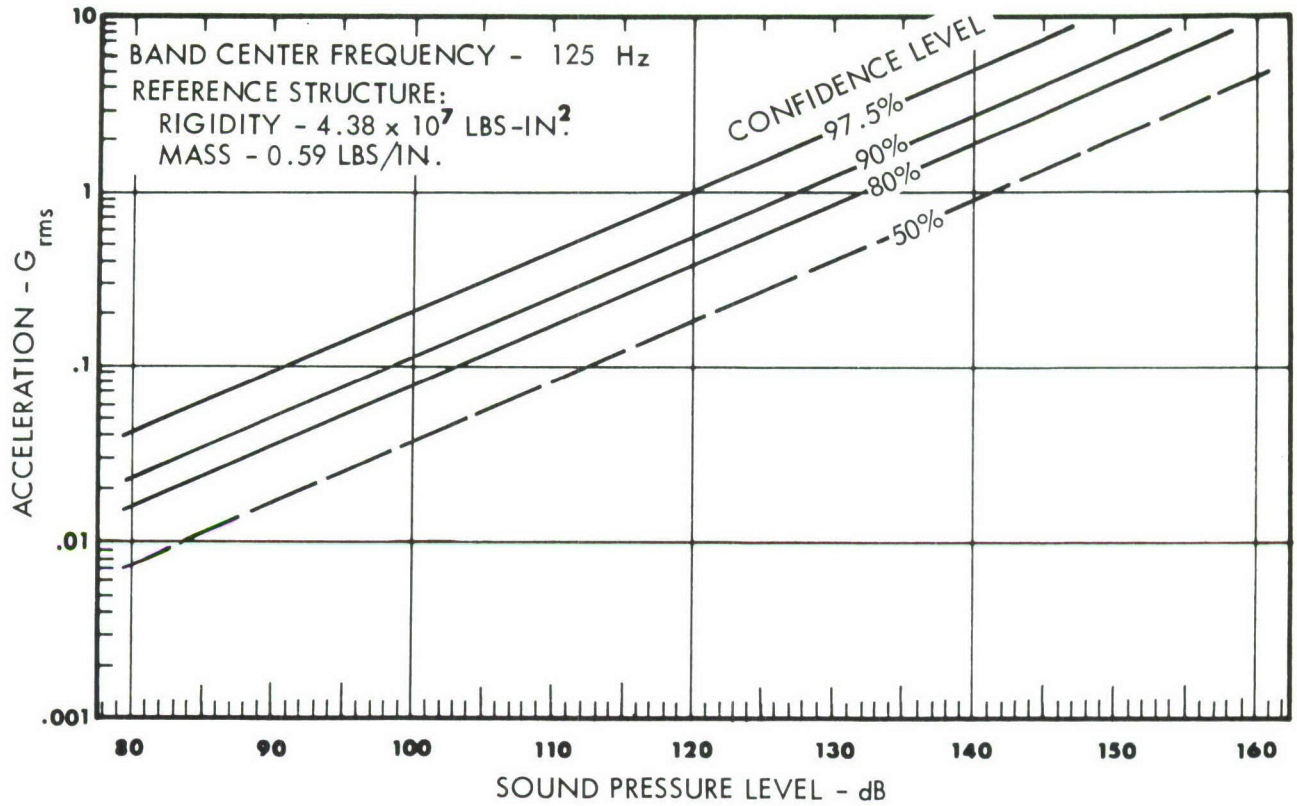


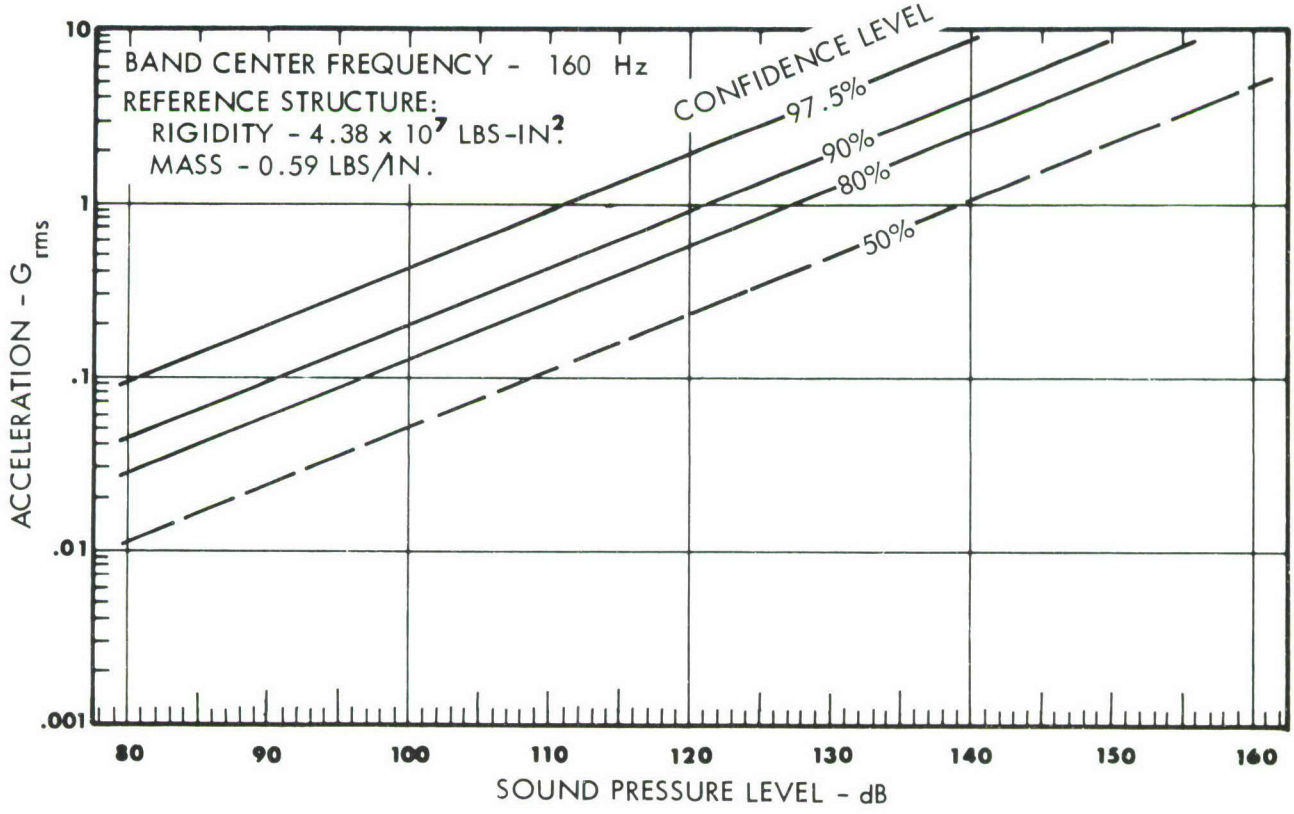


FIGURE 3. THIRD-OCTAVE BAND VIBRATION PREDICTION CHART FOR SHELL STRUCTURE; NORMAL DIRECTION; GROUND OPERATION

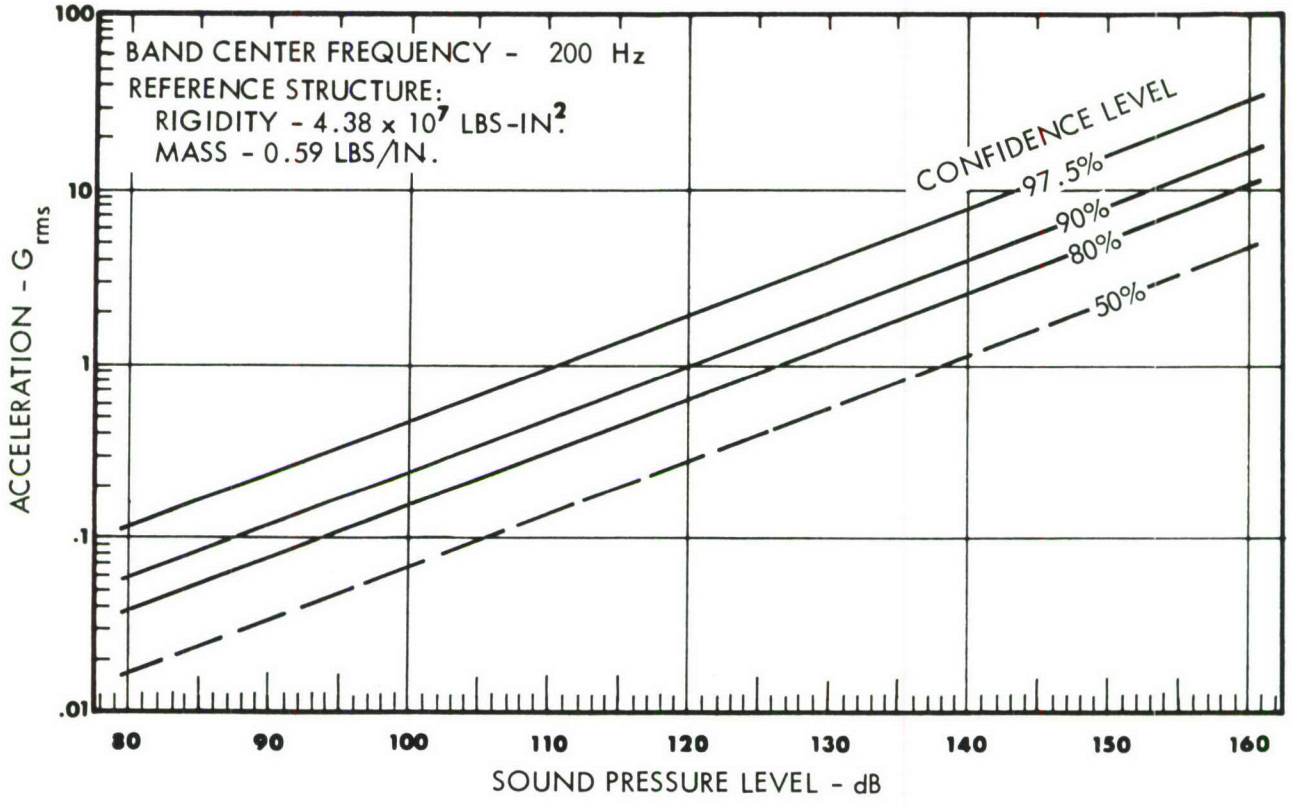


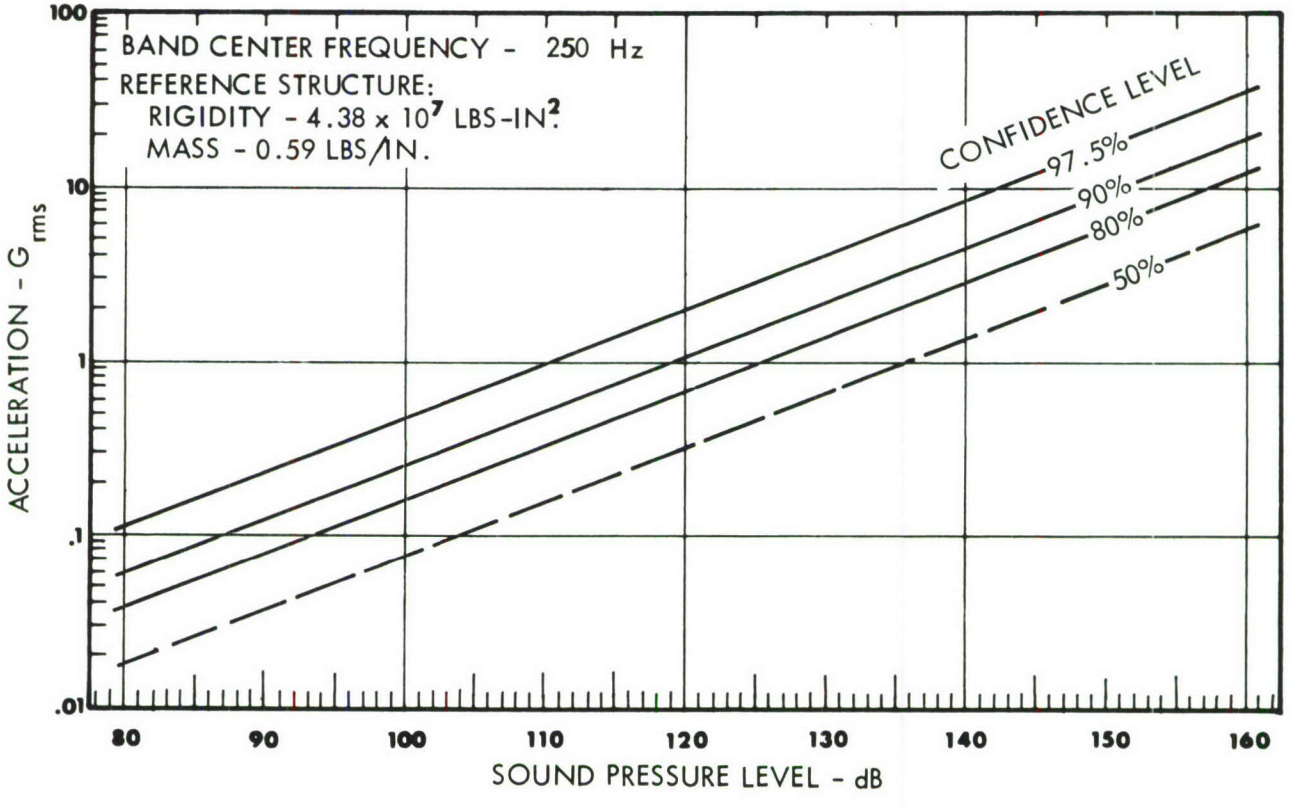


FIGURE 4. THIRD-OCTAVE BAND VIBRATION PREDICTION CHART FOR SHELL STRUCTURE; NORMAL DIRECTION; GROUND OPERATION

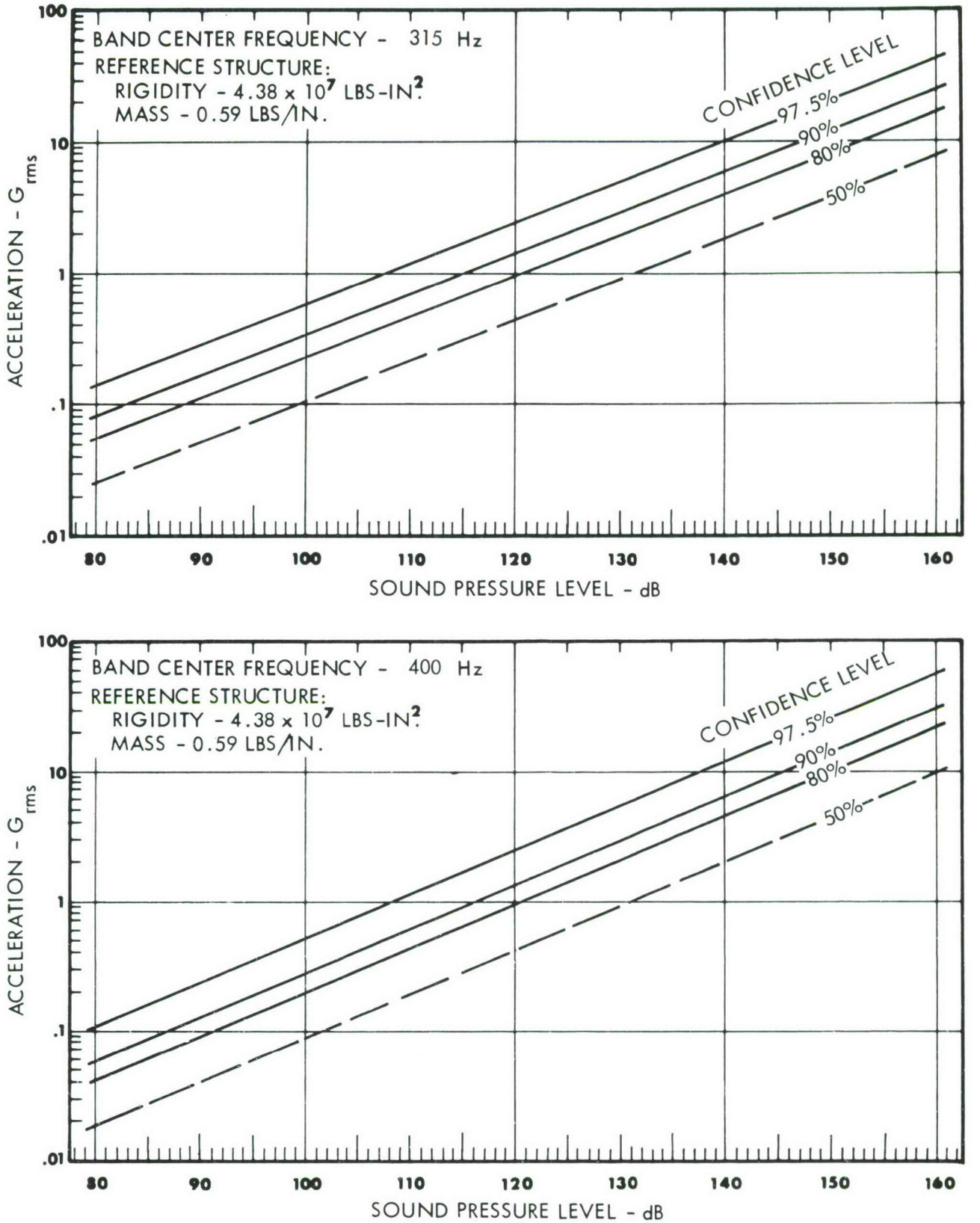


FIGURE 5. THIRD-OCTAVE BAND VIBRATION PREDICTION CHART FOR SHELL STRUCTURE; NORMAL DIRECTION; GROUND OPERATION

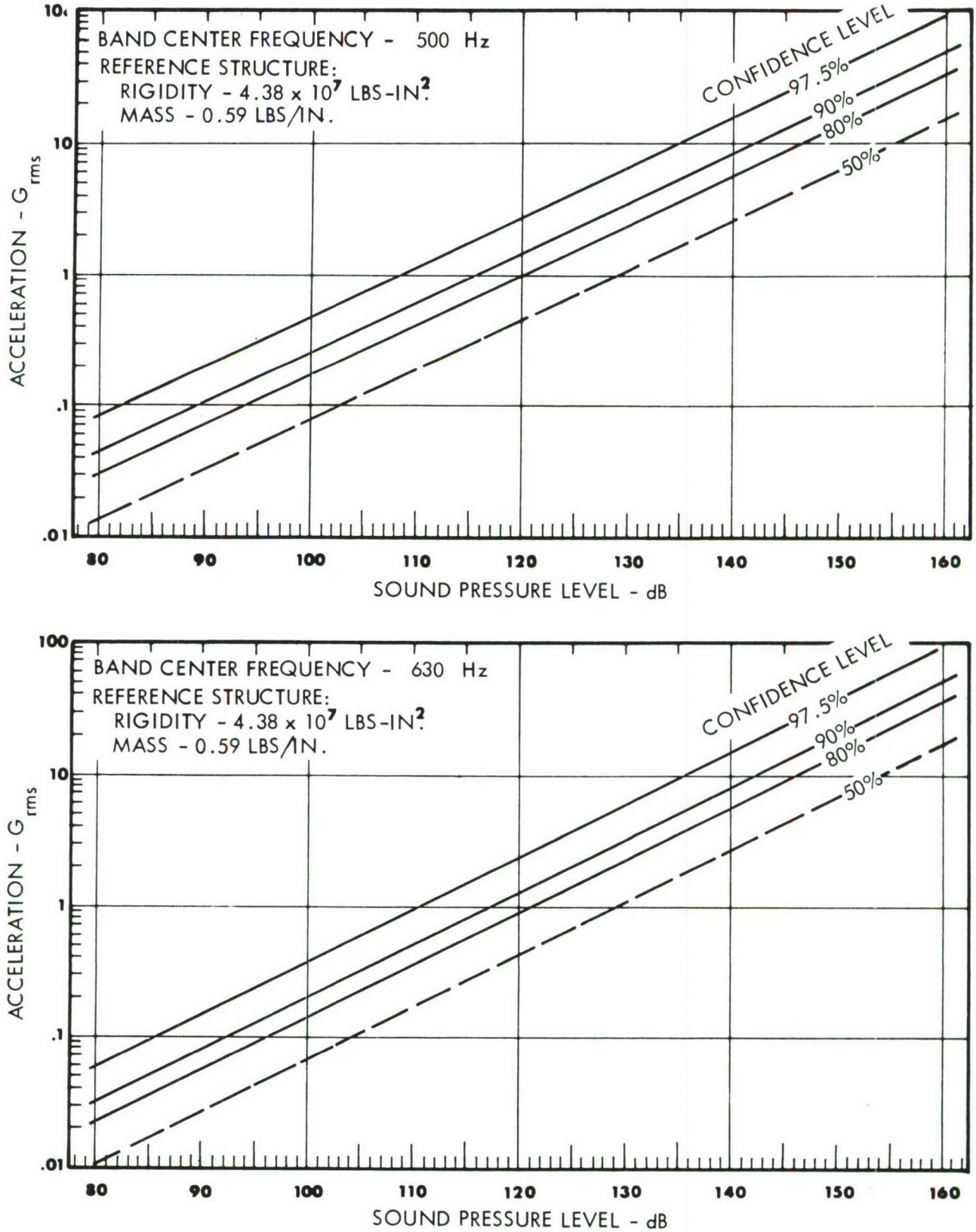


FIGURE 6. THIRD-OCTAVE BAND VIBRATION PREDICTION CHART FOR SHELL STRUCTURE; NORMAL DIRECTION; GROUND OPERATION

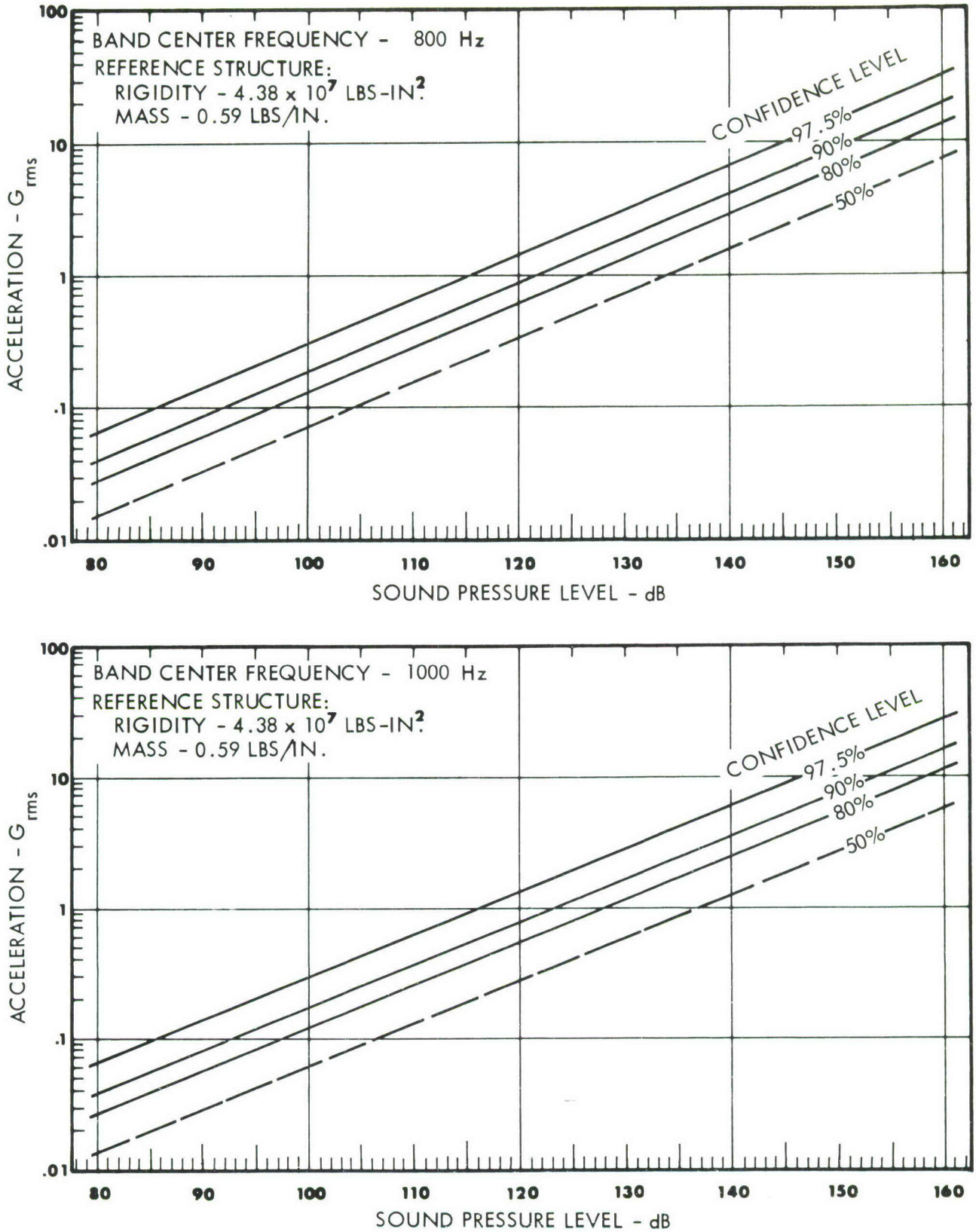


FIGURE 7. THIRD-OCTAVE BAND VIBRATION PREDICTION CHART FOR SHELL STRUCTURE; NORMAL DIRECTION; GROUND OPERATION

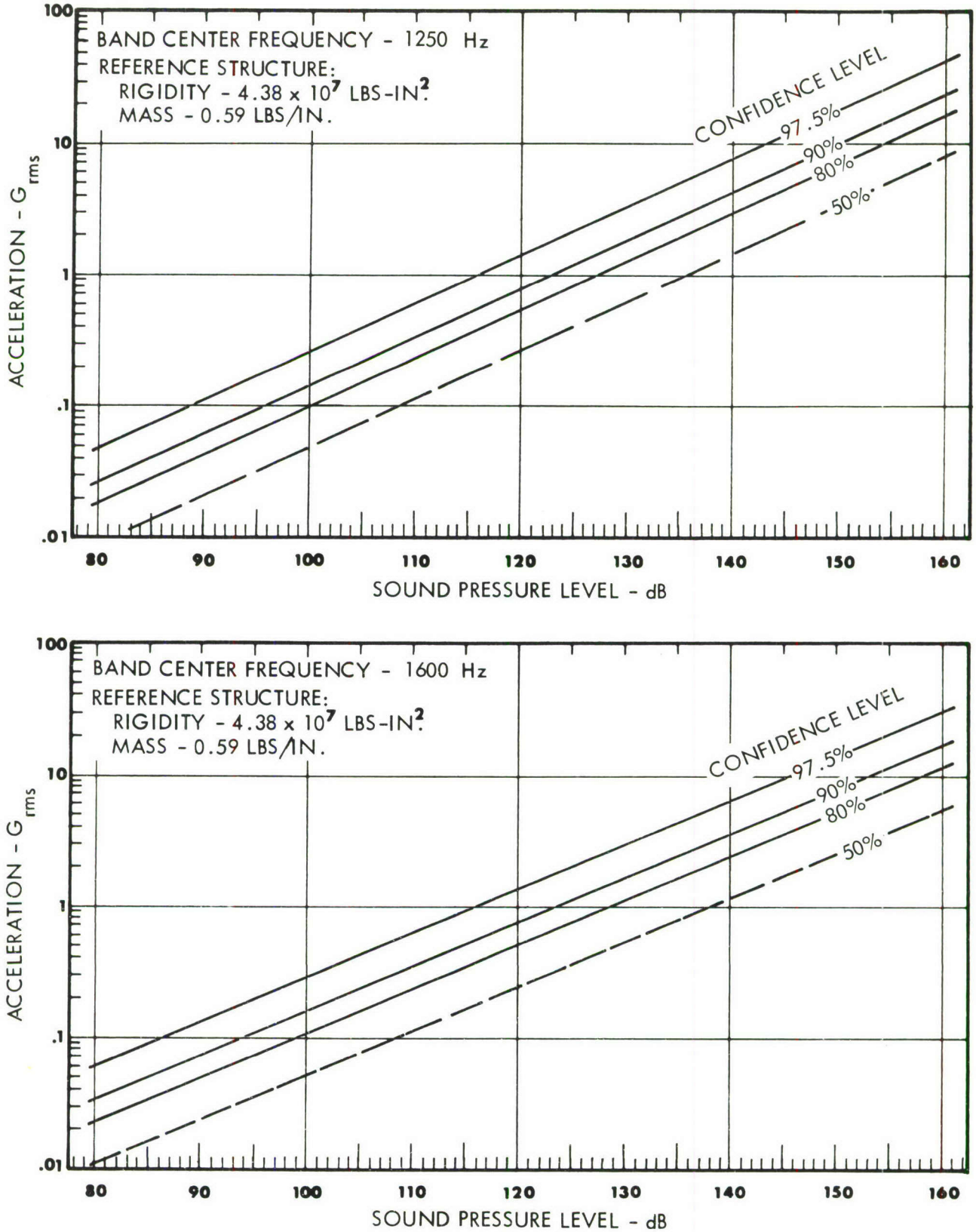


FIGURE 8. THIRD-OCTAVE BAND VIBRATION PREDICTION CHART FOR SHELL STRUCTURE; NORMAL DIRECTION; GROUND OPERATION

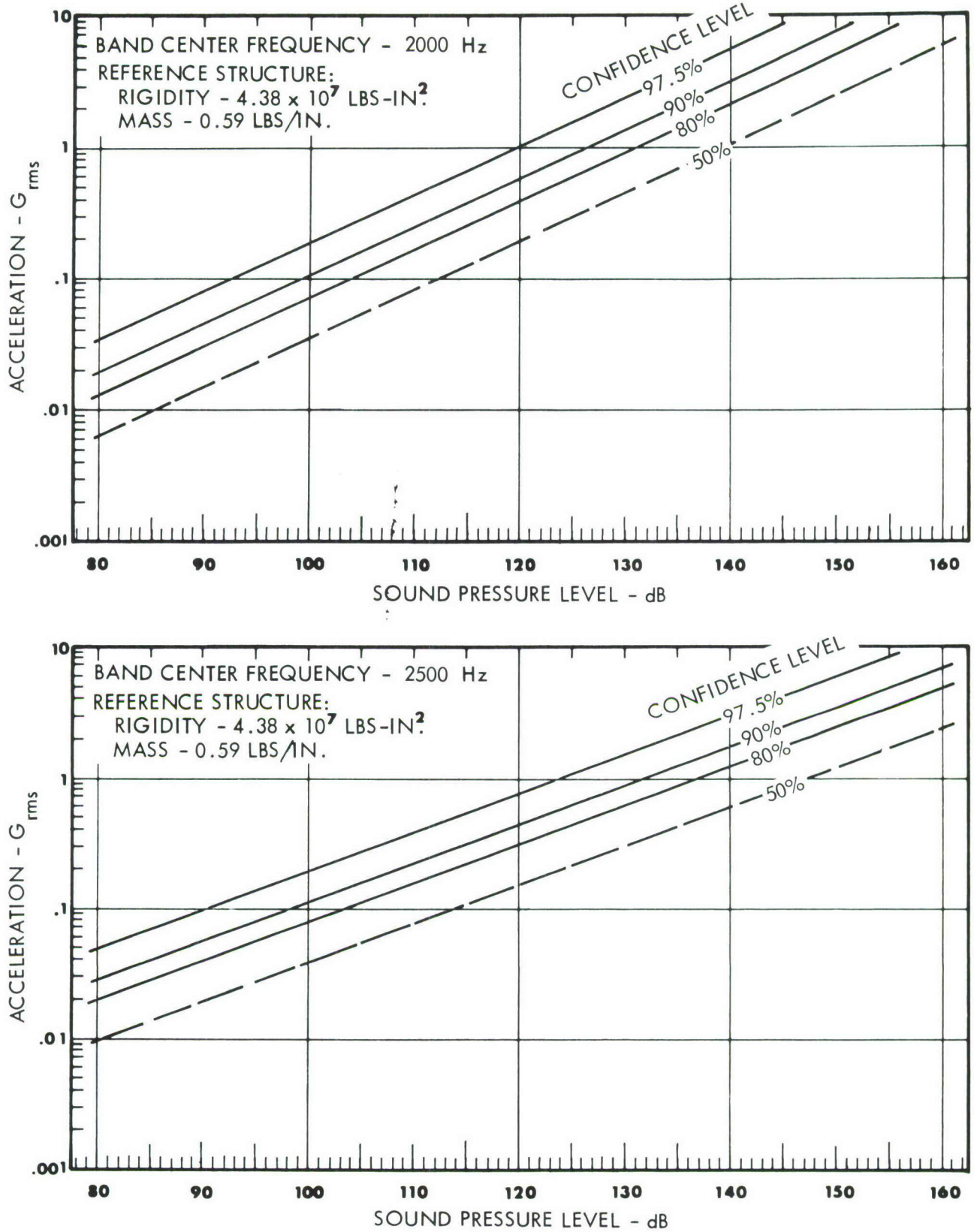


FIGURE 9. THIRD-OCTAVE BAND VIBRATION PREDICTION CHART FOR SHELL STRUCTURE; NORMAL DIRECTION; GROUND OPERATION

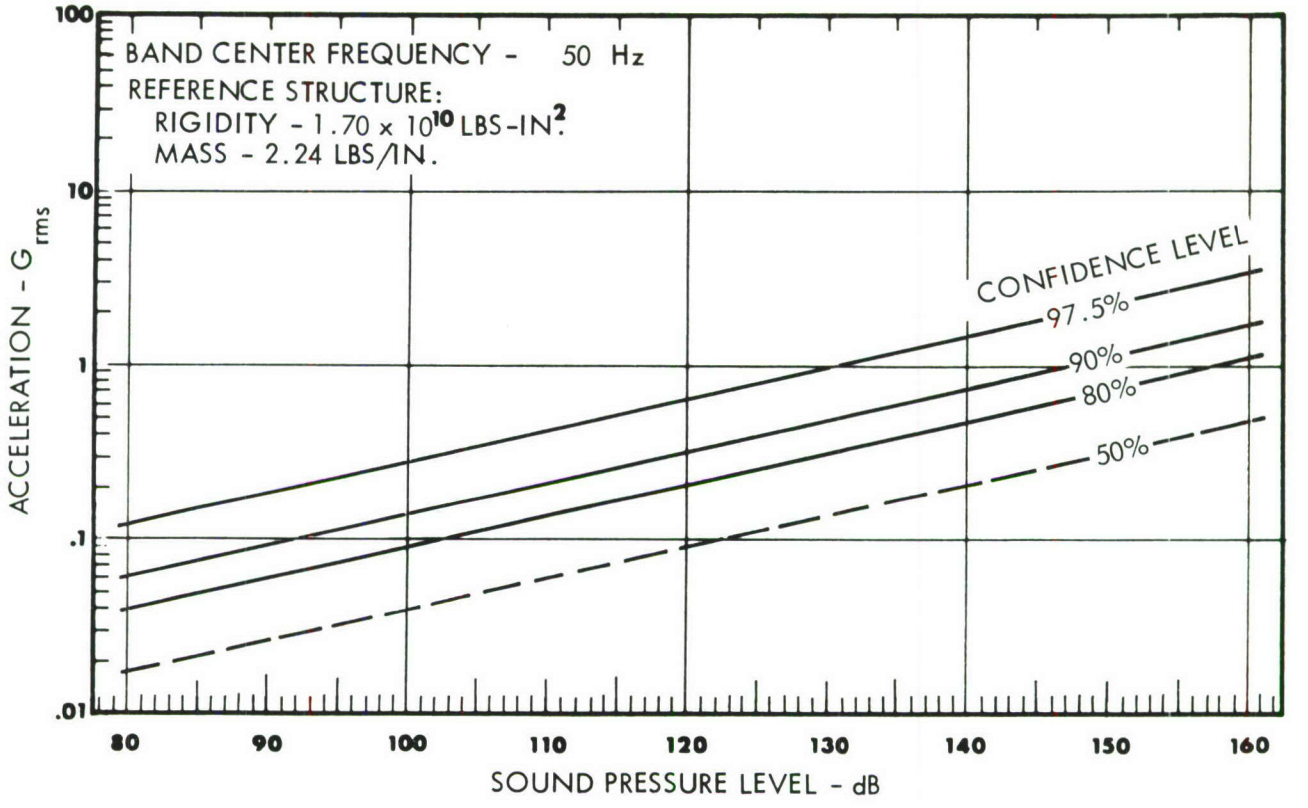


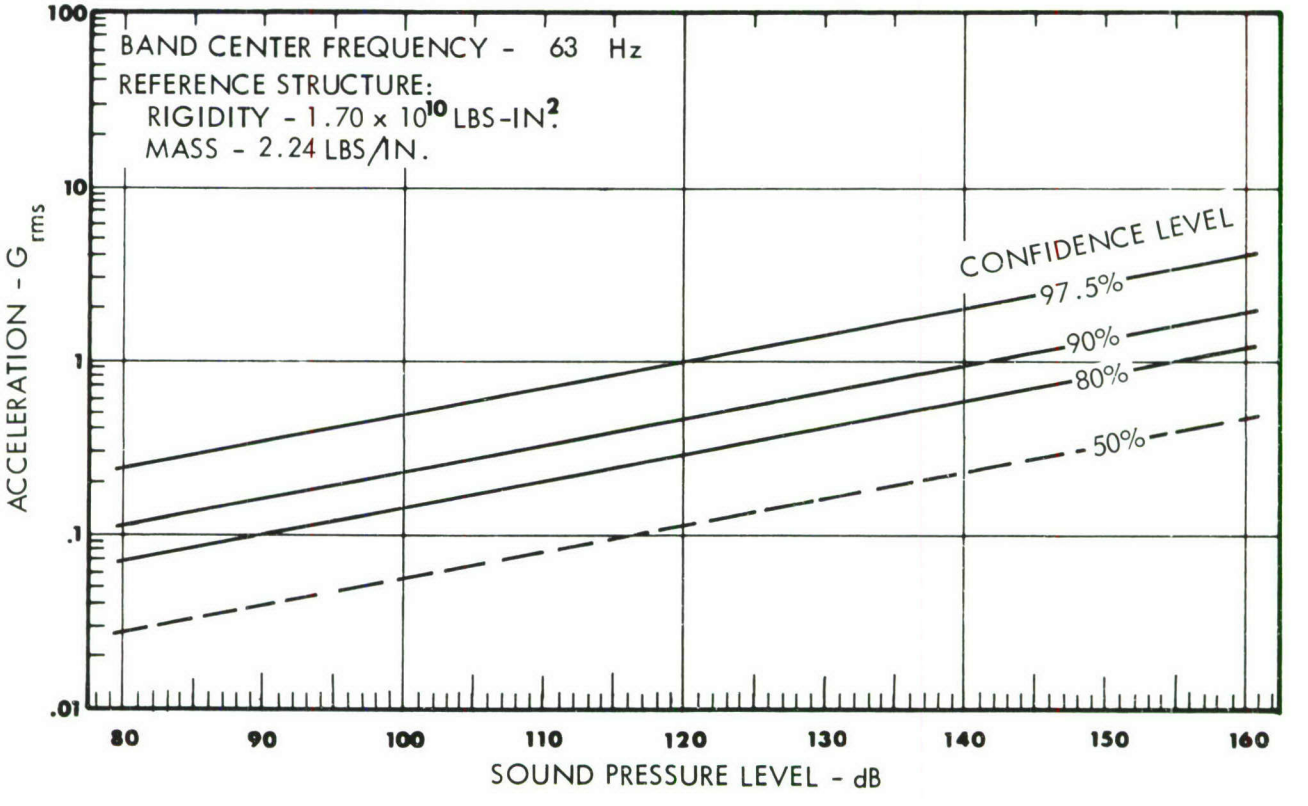


FIGURE 10. THIRD-OCTAVE BAND VIBRATION PREDICTION CHART FOR BOX STRUCTURE; NORMAL DIRECTION; GROUND OPERATION

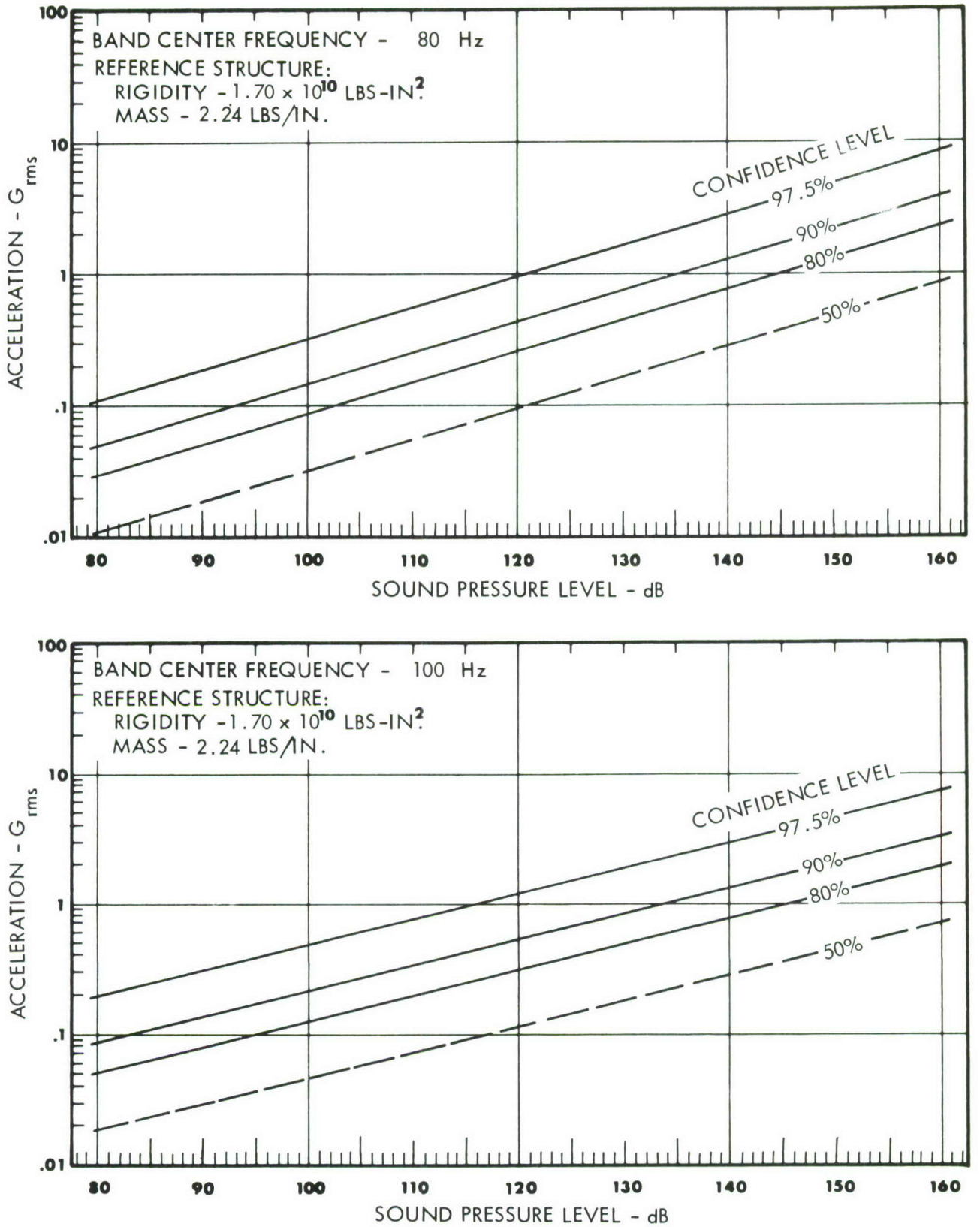


FIGURE 11. THIRD-OCTAVE BAND VIBRATION PREDICTION CHART FOR BOX STRUCTURE; NORMAL DIRECTION; GROUND OPERATION

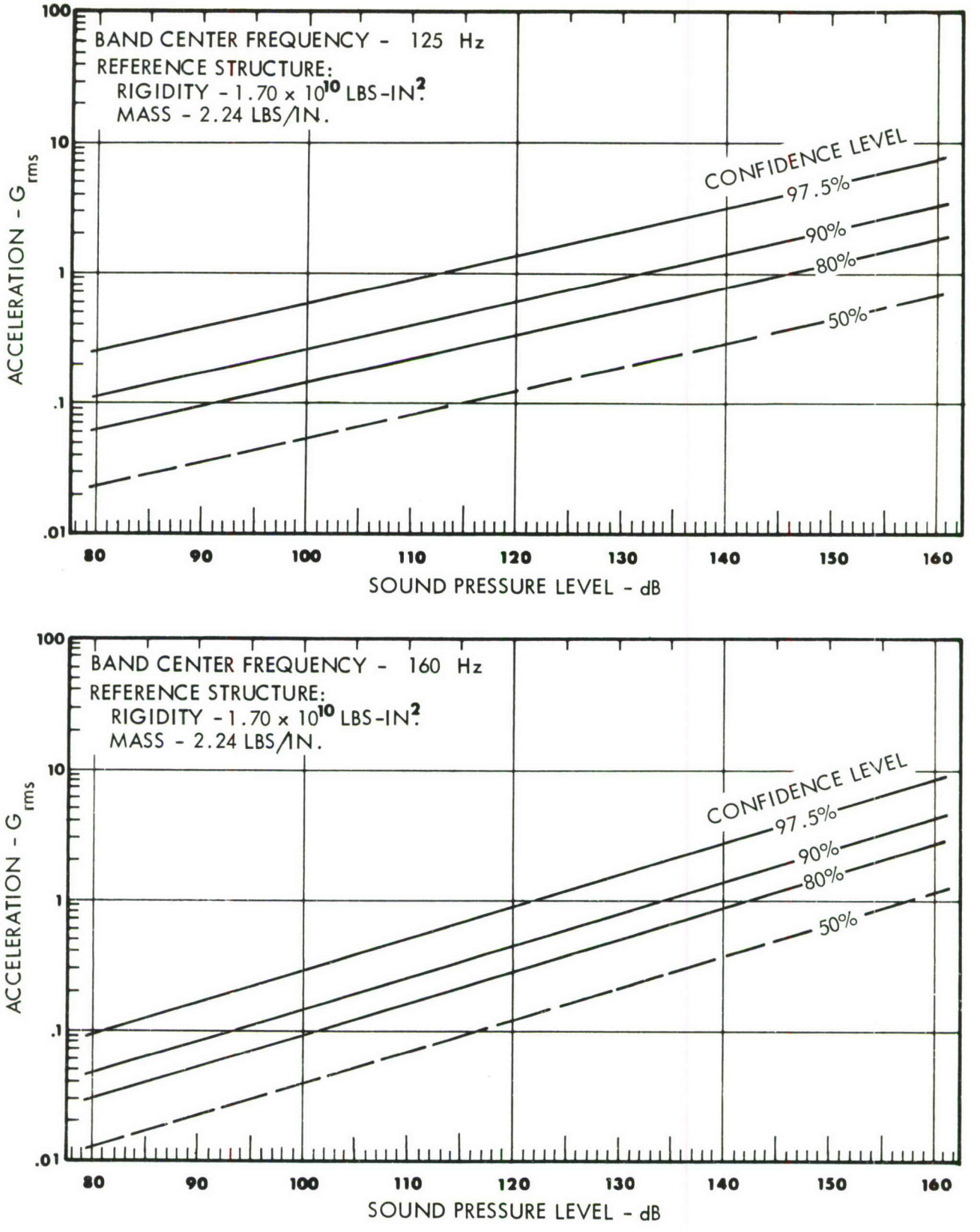


FIGURE 12. THIRD-OCTAVE BAND VIBRATION PREDICTION CHART FOR BOX STRUCTURE; NORMAL DIRECTION; GROUND OPERATION

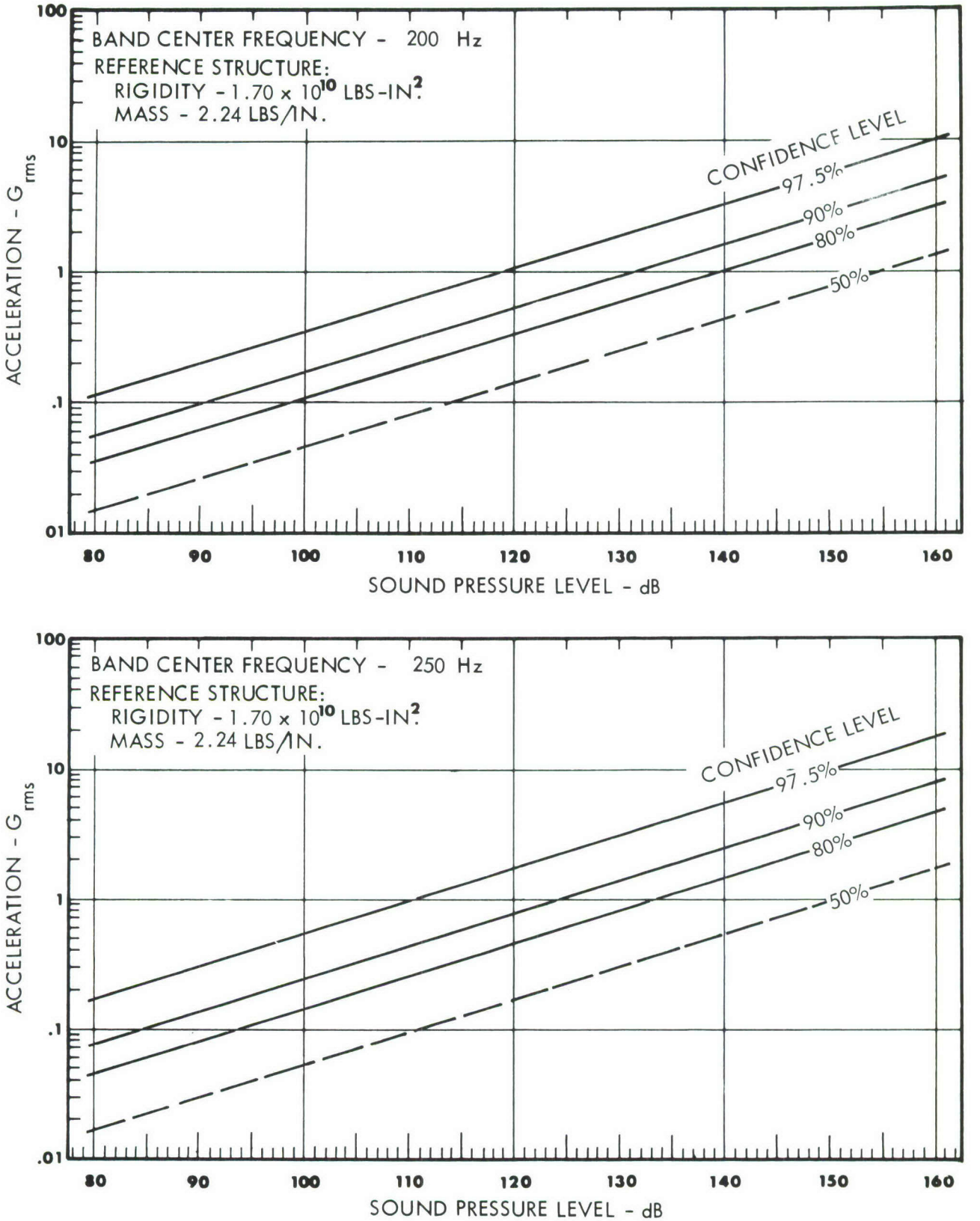


FIGURE 13. THIRD-OCTAVE BAND VIBRATION PREDICTION CHART FOR BOX STRUCTURE; NORMAL DIRECTION; GROUND OPERATION

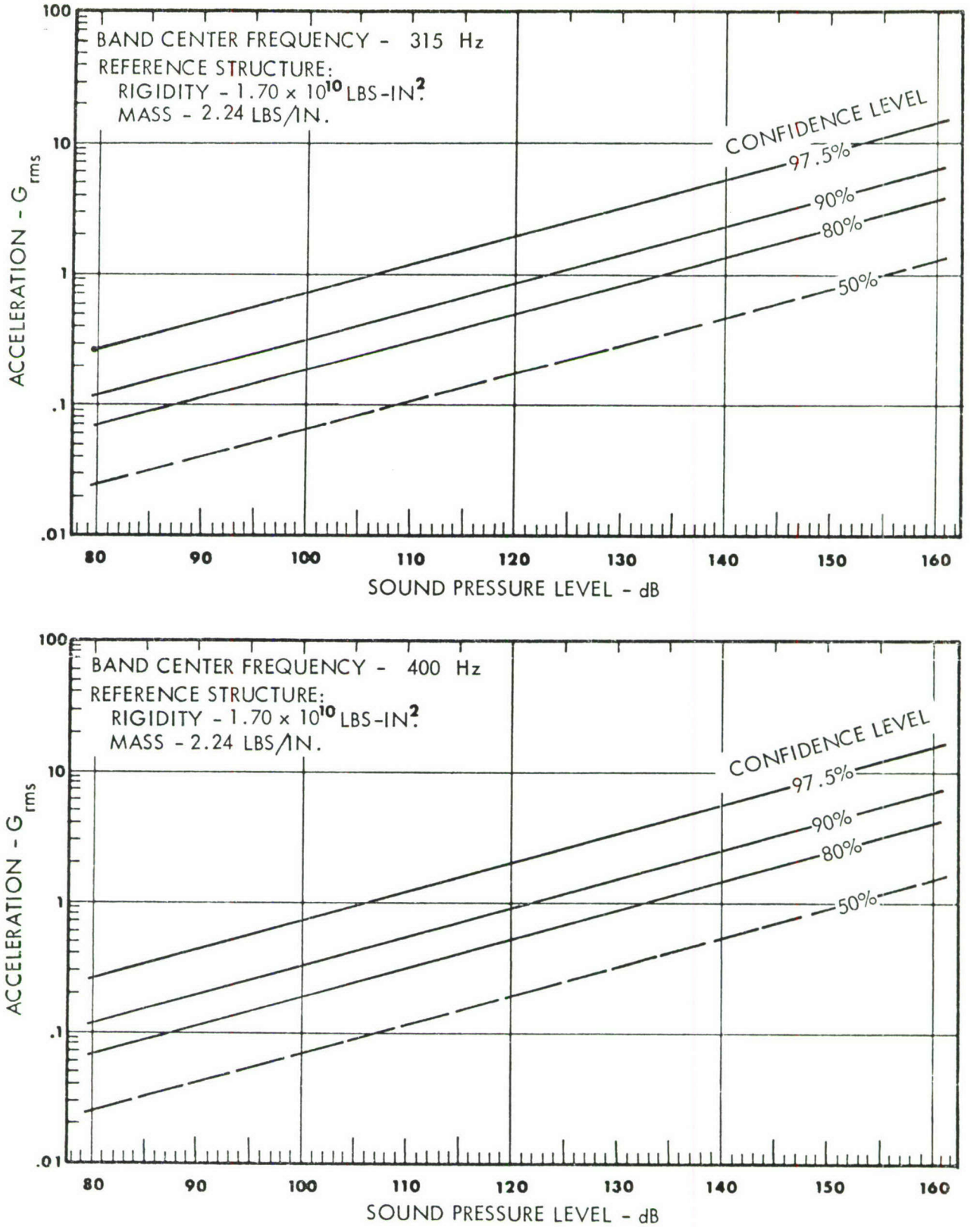


FIGURE 14. THIRD-OCTAVE BAND VIBRATION PREDICTION CHART FOR BOX STRUCTURE; NORMAL DIRECTION; GROUND OPERATION

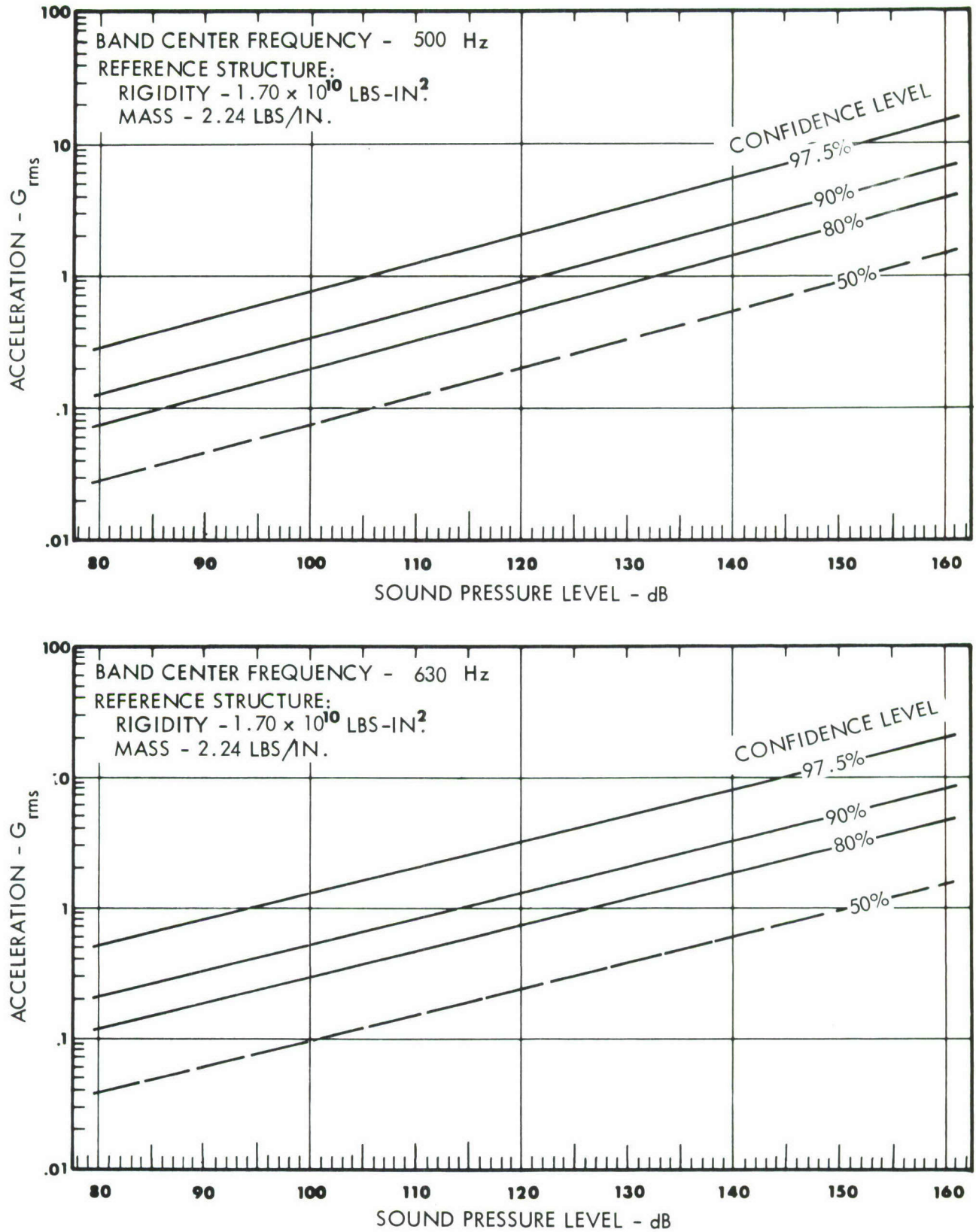


FIGURE 15. THIRD-OCTAVE BAND VIBRATION PREDICTION CHART FOR BOX STRUCTURE; NORMAL DIRECTION; GROUND OPERATION

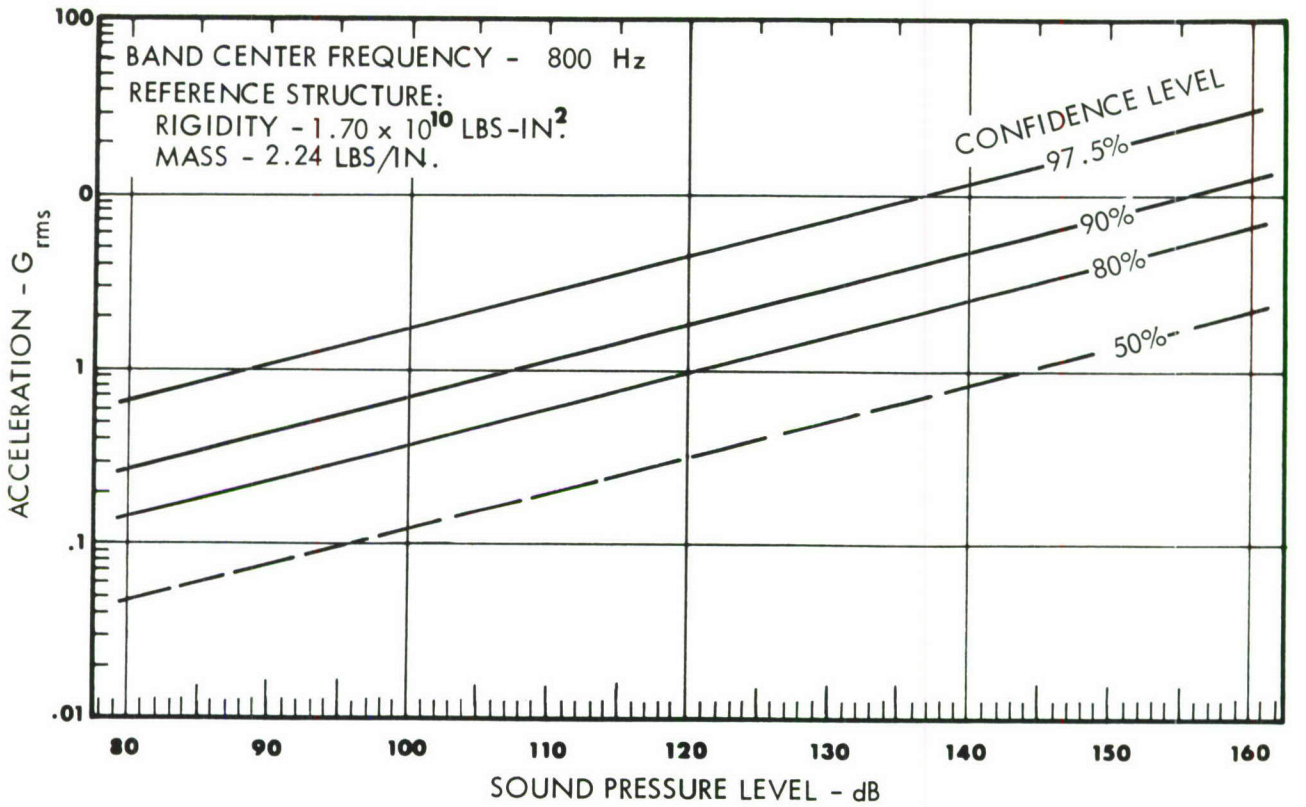


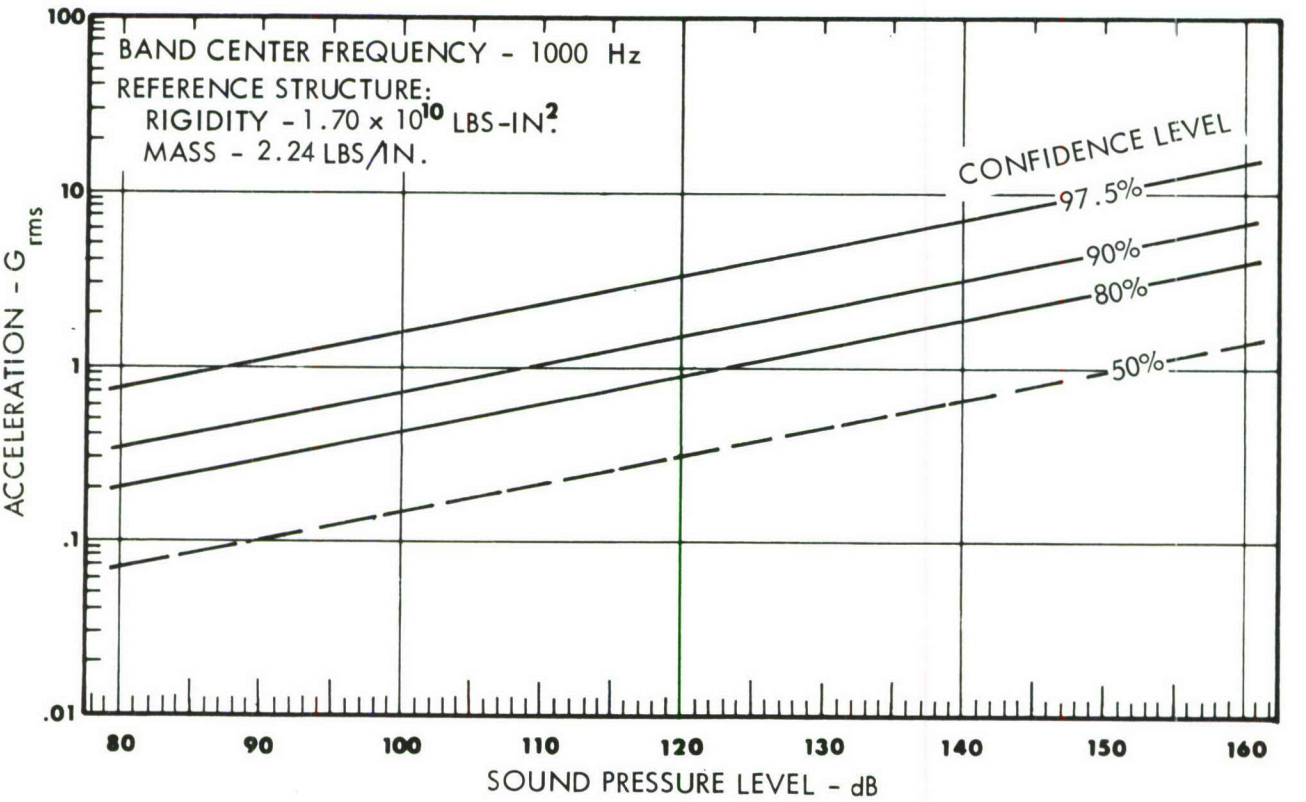


FIGURE 16. THIRD-OCTAVE BAND VIBRATION PREDICTION CHART FOR BOX STRUCTURE; NORMAL DIRECTION; GROUND OPERATION

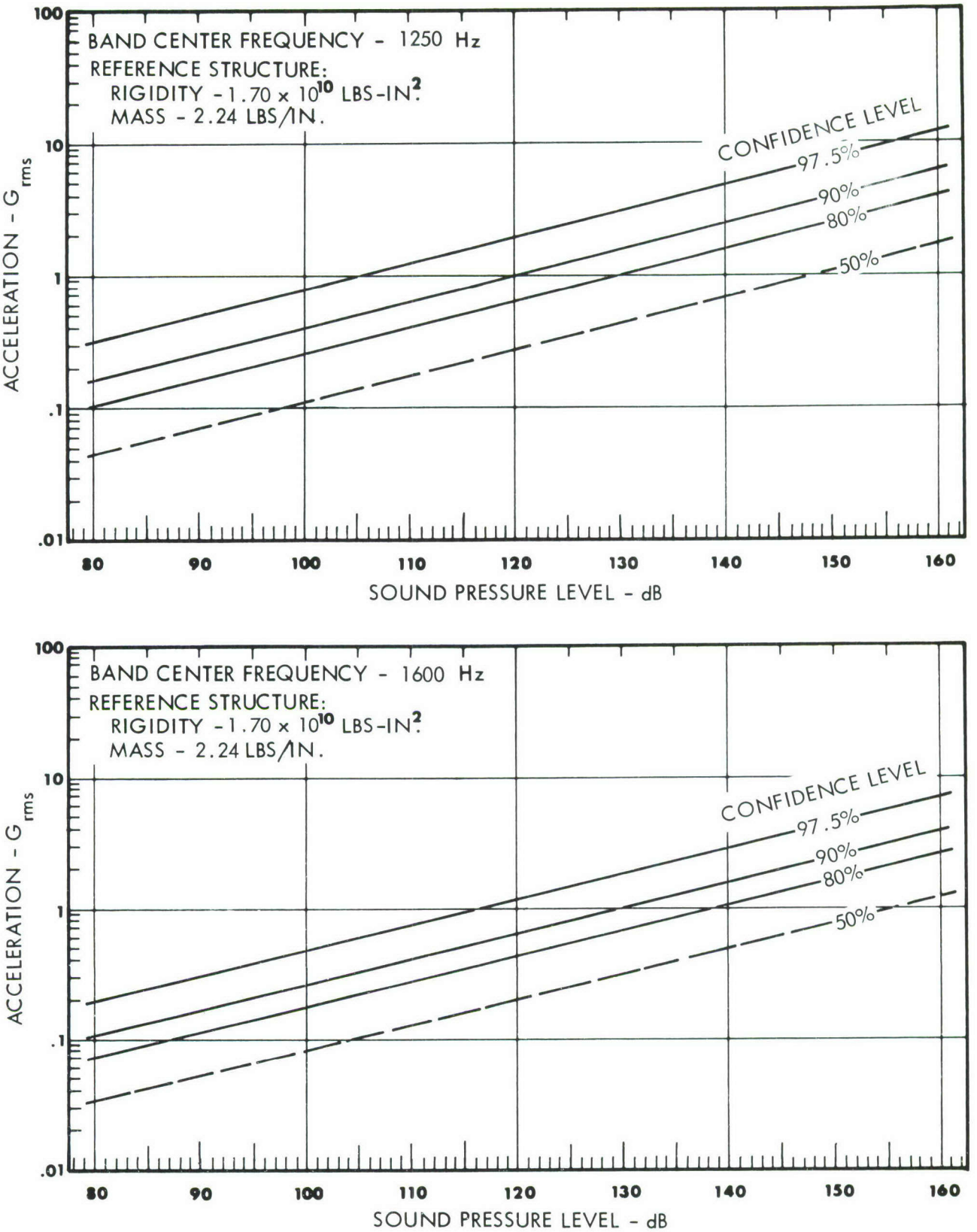


FIGURE 17. THIRD-OCTAVE BAND VIBRATION PREDICTION CHART FOR BOX STRUCTURE; NORMAL DIRECTION; GROUND OPERATION

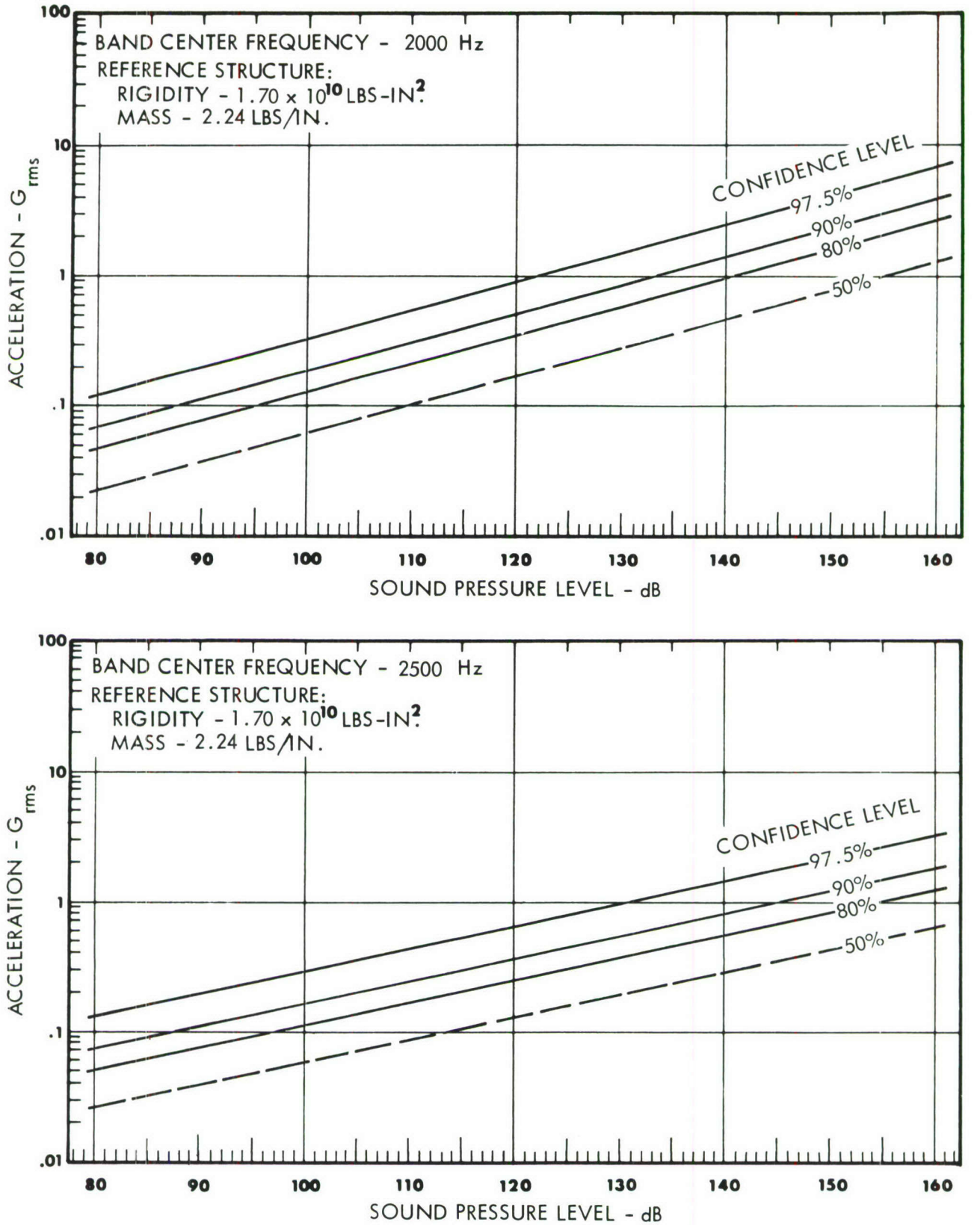


FIGURE 18. THIRD-OCTAVE BAND VIBRATION PREDICTION CHART FOR BOX STRUCTURE; NORMAL DIRECTION; GROUND OPERATION

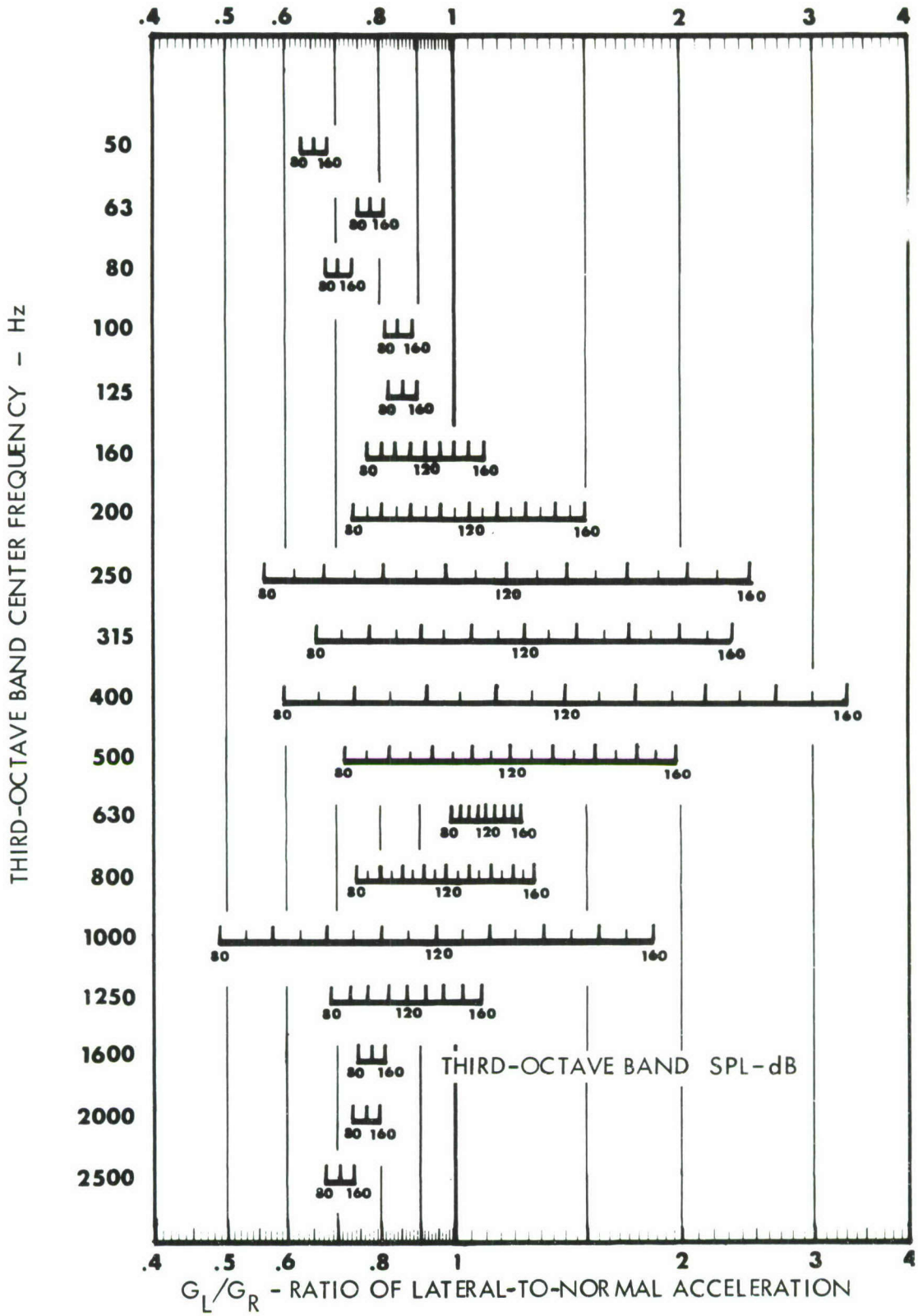


FIGURE 19. LATERAL VIBRATION PREDICTION CHART

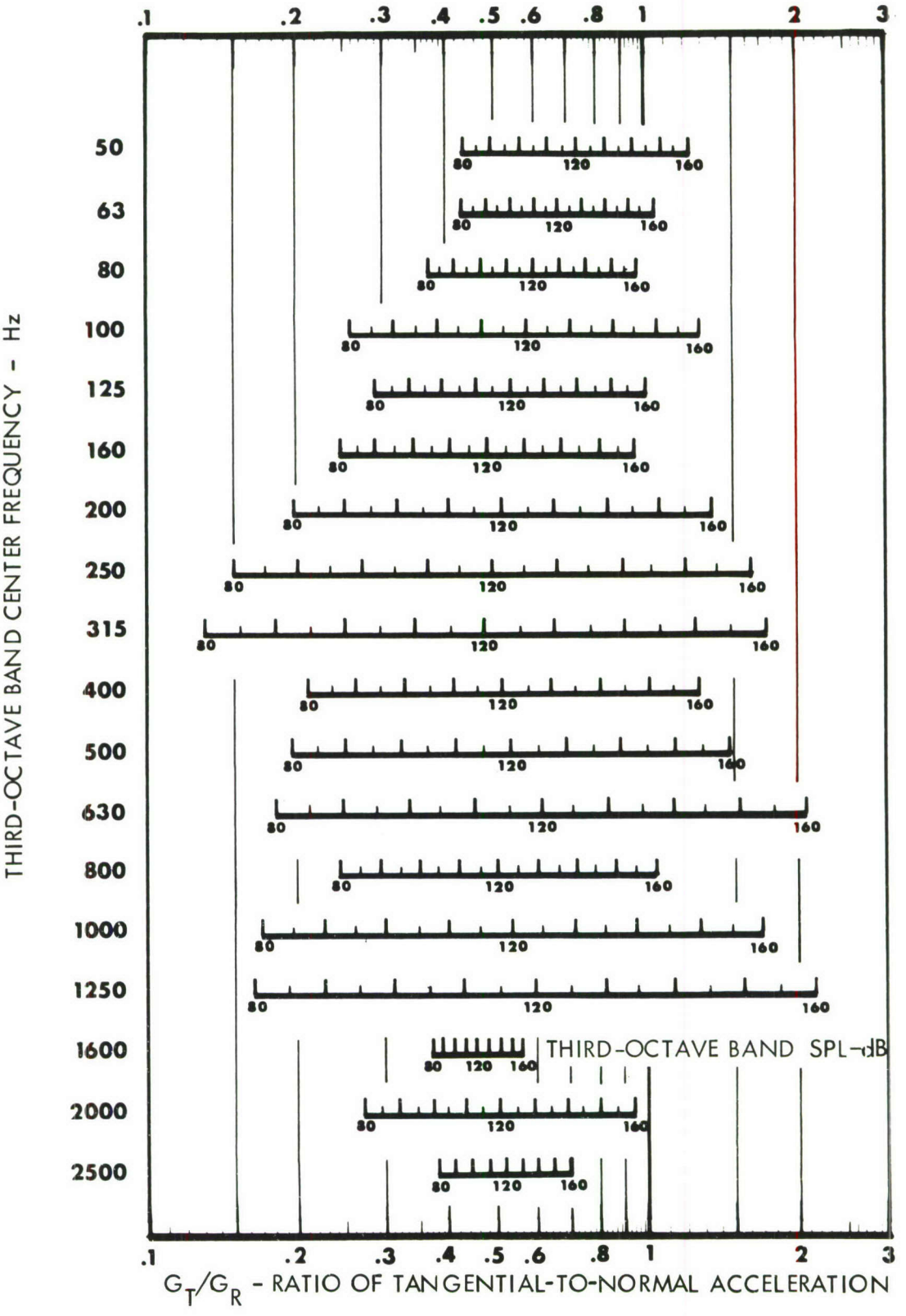


FIGURE 20. TANGENTIAL VIBRATION PREDICTION CHART

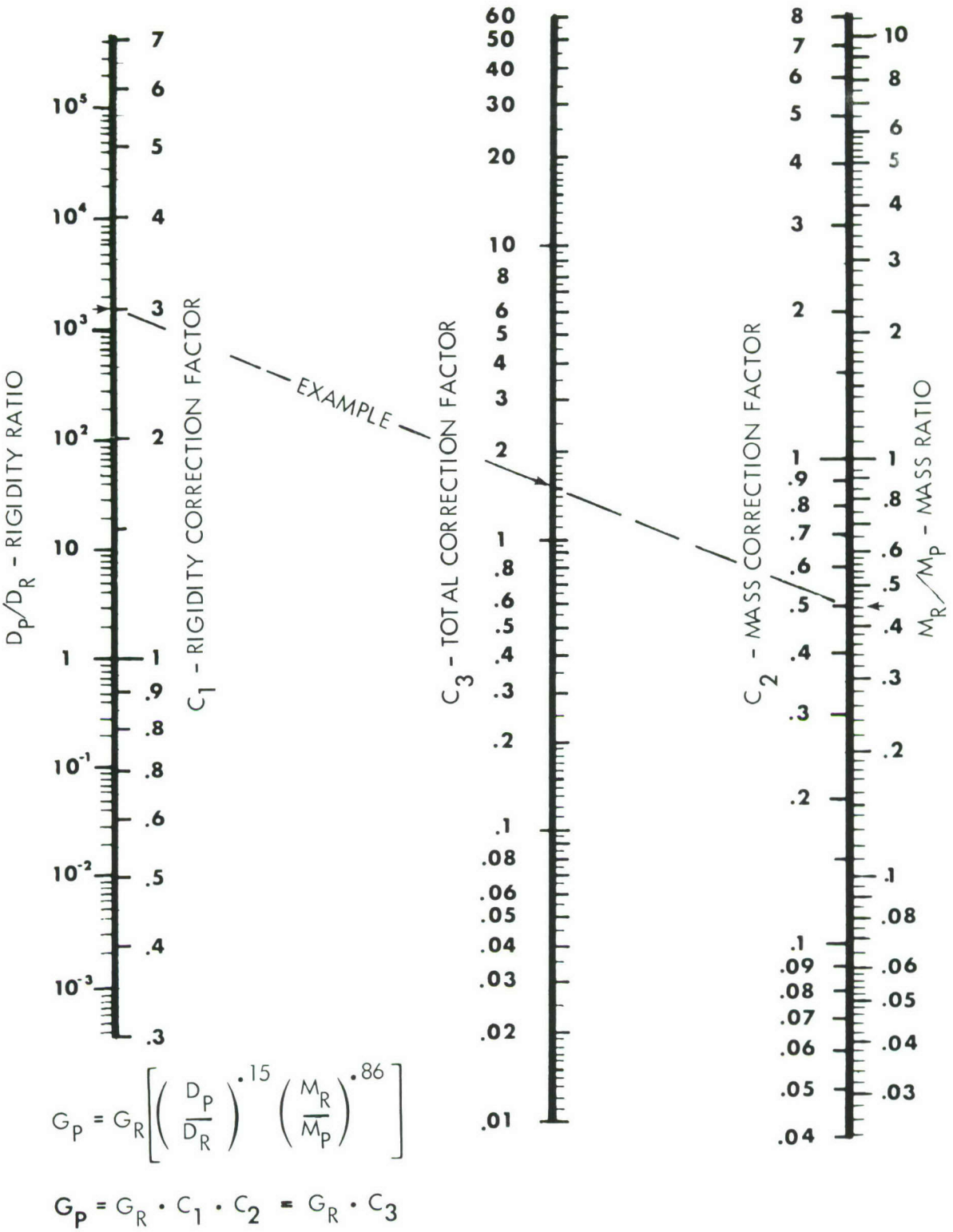


FIGURE 21. MASS AND RIGIDITY CORRECTION NOMOGRAPH

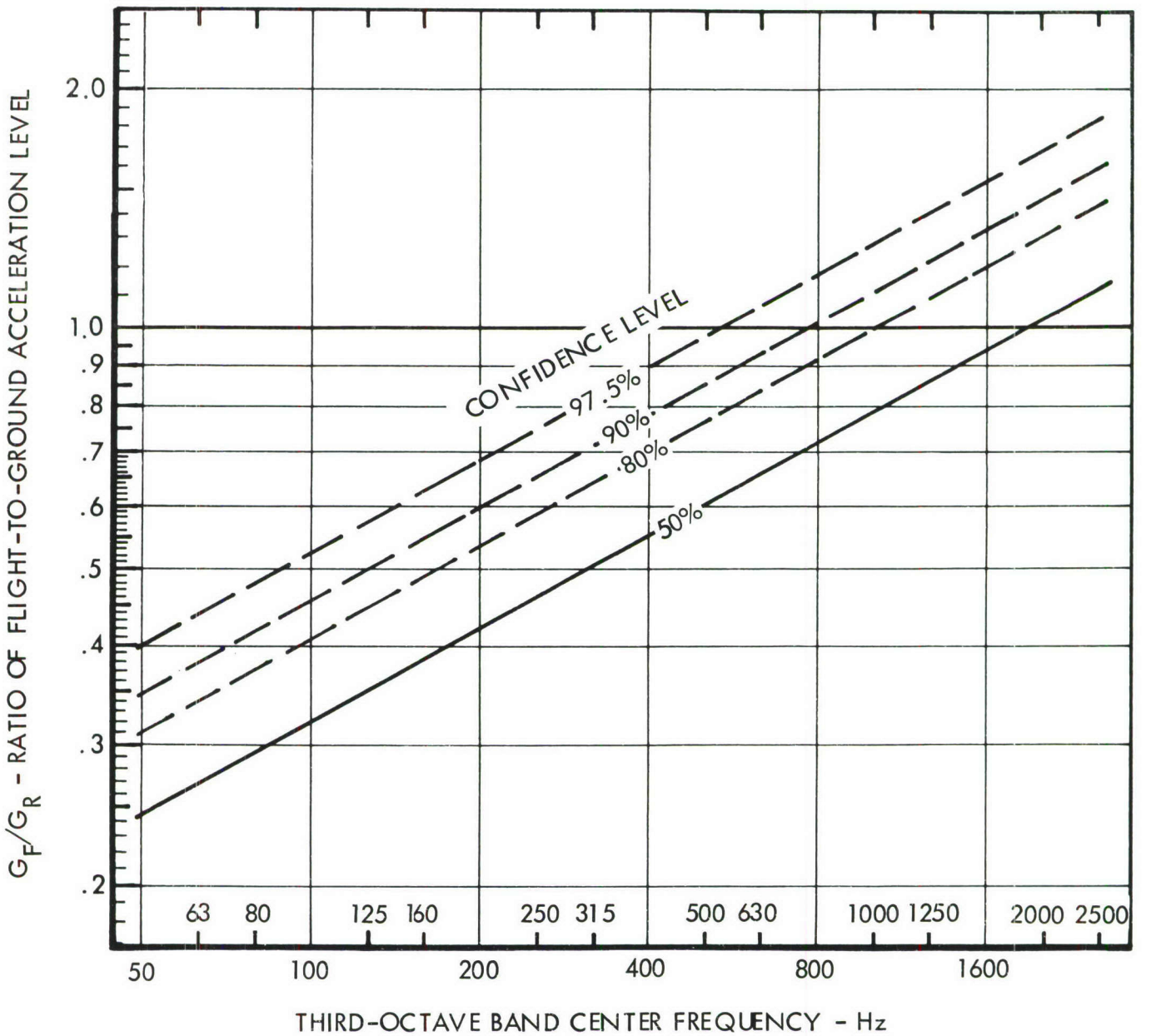


FIGURE 22. FLIGHT VIBRATION PREDICTION CHART

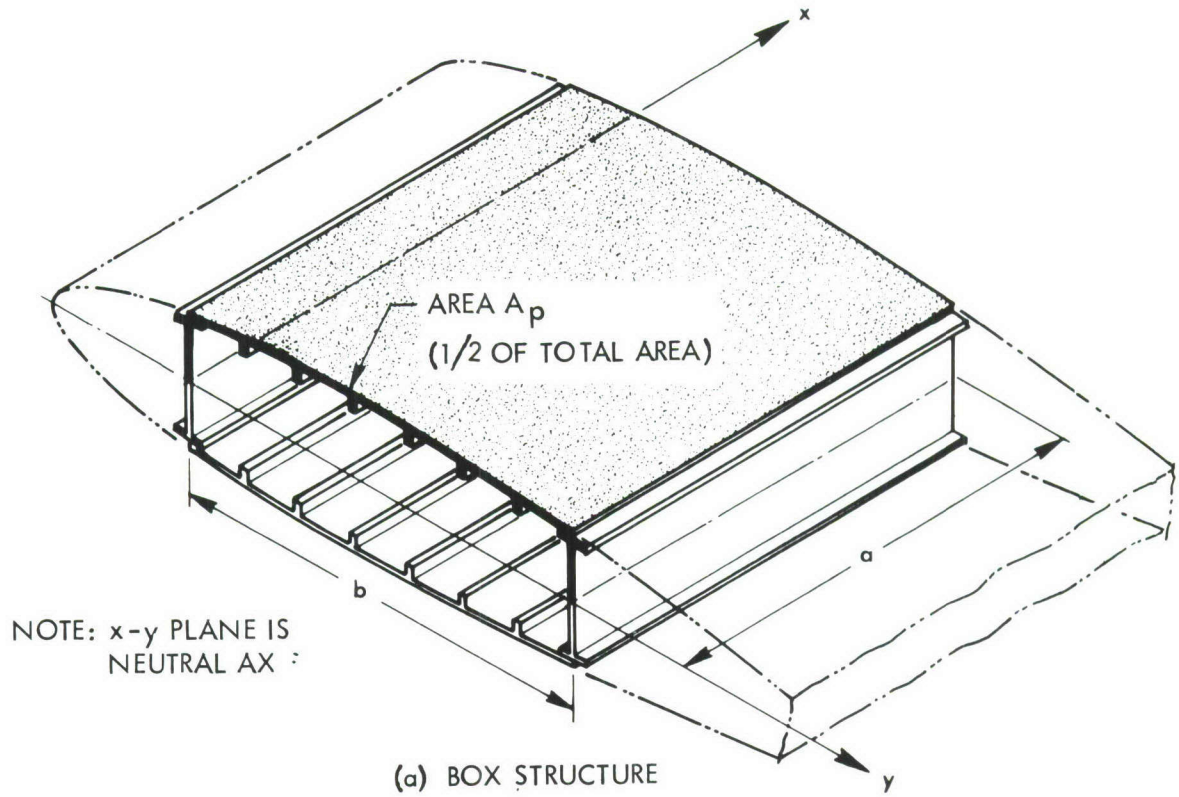


(a) BOX STRUCTURE

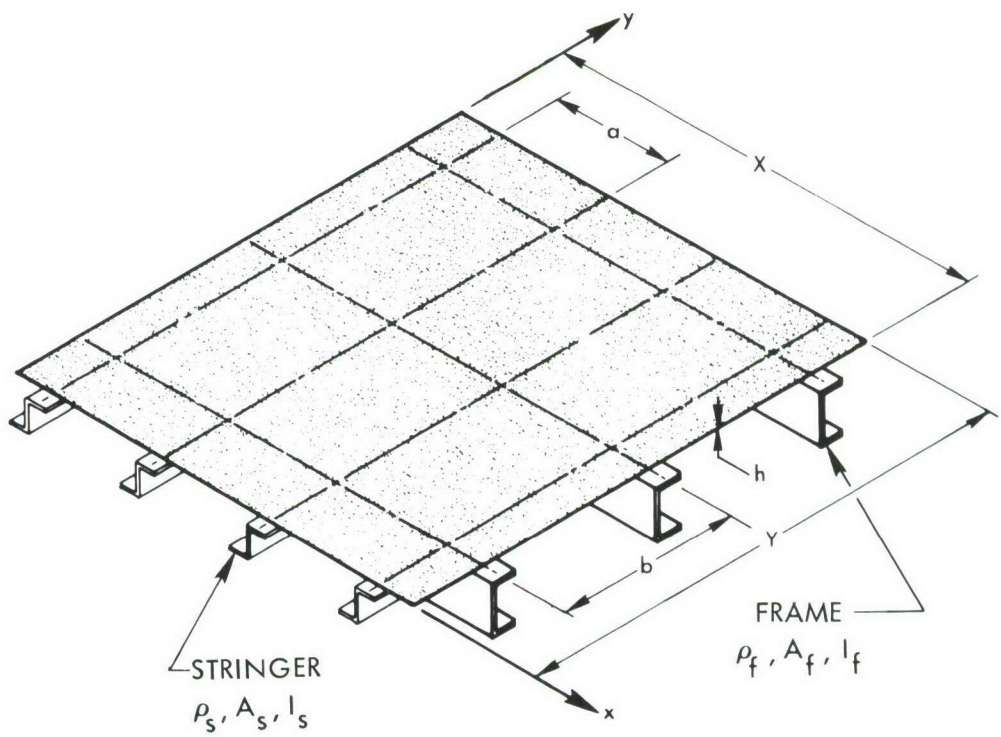


(b) SHELL STRUCTURE

FIGURE 23. COORDINATE SYSTEM FOR SHELL AND BOX STRUCTURE

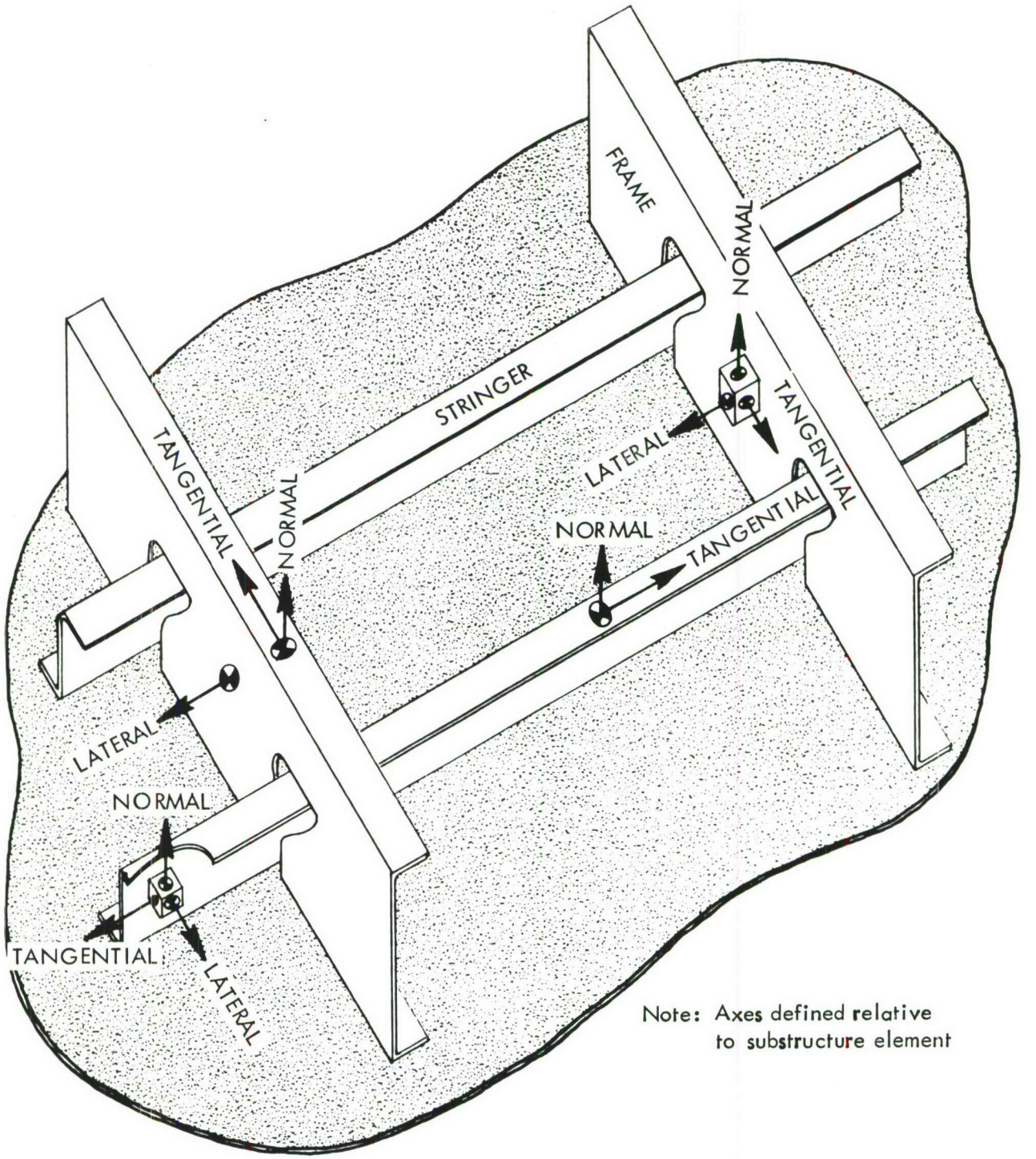


FIGURE 24. AIRCRAFT AND PANEL AXIS DEFINITION

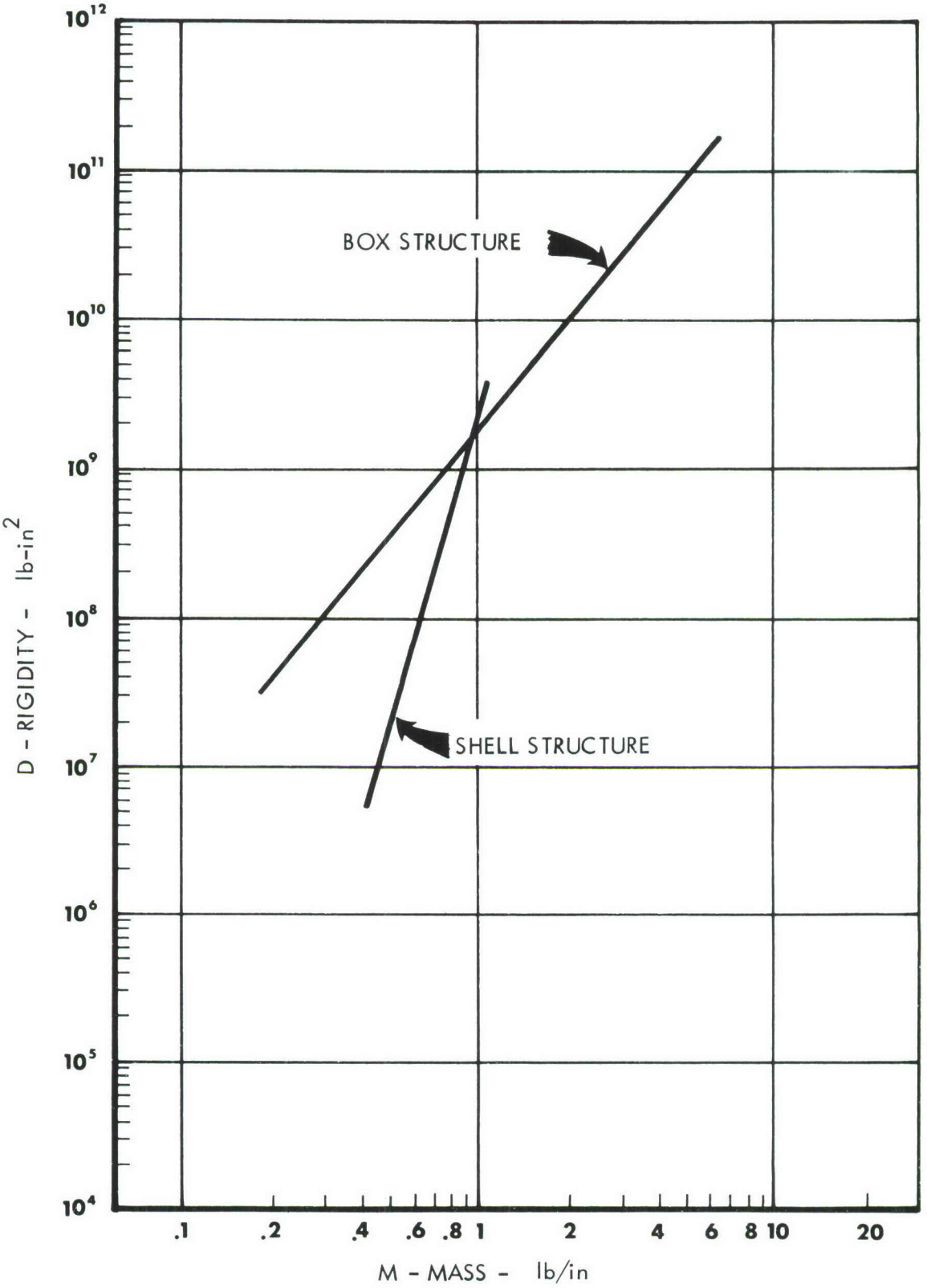


FIGURE 25. MASS AND RIGIDITY CORRELATION
AIRCRAFT SHELL AND BOX STRUCTURE

TABLE I — HYPOTHETICAL AIRCRAFT VIBRATION PREDICTION

FUSELAGE - TAKEOFF

| | | THIRD-OCTAVE BAND CENTER FREQUENCY - Hz | | | | | | | | | | | | | | | | | |
|---|---|---|---|---|---|---|---|---|---|---|---|---|---|---|---|---|---|---|---|
| | | 50 | 63 | 80 | 100 | 125 | 160 | 200 | 250 | 315 | 400 | 500 | 630 | 800 | 1000 | 1250 | 1600 | 2000 | 2500 |
| 1 | $G_{rms}$ Ref Shell | .14 | .22 | .27 | .30 | .51 | .98 | 1.2 | 1.25 | 2.1 | 2.1 | 3.0 | 3.0 | 1.9 | 1.7 | 1.7 | 1.3 | 1.25 | 1.1 |
| 2 | $C_3$ | .90 | .90 | .90 | .90 | .90 | .90 | .90 | .90 | .90 | .90 | .90 | .90 | .90 | .90 | .90 | .90 | .90 | .90 |
| 3 | $G_{rms}$ Fus Norm | .13 | .20 | .24 | .27 | .46 | .88 | 1.08 | 1.13 | 1.89 | 1.89 | 2.7 | 2.7 | 1.71 | 1.53 | 1.53 | 1.17 | 1.13 | .99 |
| 4 | $G_L/G_R$ | .65 | .77 | .70 | .84 | .86 | .93 | 1.07 | 1.24 | 1.33 | 1.58 | 1.33 | 1.13 | 1.05 | 1.14 | .91 | .78 | .77 | .71 |
| 5 | $G_{rms}$ Fus Lat | .084 | .15 | .17 | .23 | .40 | .82 | 1.16 | 1.40 | 2.51 | 2.99 | 3.59 | 3.05 | 1.80 | 1.74 | 1.39 | .91 | .87 | .70 |
| 6 | $G_T/G_R$ | .66 | .64 | .58 | .56 | .54 | .49 | .54 | .54 | .56 | .59 | .65 | .82 | .61 | .74 | .81 | .47 | .58 | .58 |
| 7 | $G_{rms}$ Fus Tan | .086 | .13 | .14 | .15 | .25 | .43 | .58 | .61 | 1.06 | 1.11 | 1.76 | 2.21 | 1.04 | 1.13 | 1.24 | .55 | .66 | .57 |
| 8 | $G_{rms}$ Fus Worst | .13 | .20 | .24 | .27 | .46 | .88 | 1.16 | 1.40 | 2.51 | 2.99 | 3.59 | 3.05 | 1.80 | 1.74 | 1.53 | 1.17 | 1.13 | .99 |

FUSELAGE - CRUISE

| | | | | | | | | | | | | | | | | | | | |
|---|---|---|---|---|---|---|---|---|---|---|---|---|---|---|---|---|---|---|---|
| 9 | $G_{rms}$ Ref Shell | .095 | .16 | .21 | .27 | .56 | 1.1 | 1.3 | 1.7 | 2.1 | 1.6 | 1.5 | 1.1 | .64 | .50 | .40 | .36 | .25 | .21 |
| 10 | $C_3$ | .90 | .90 | .90 | .90 | .90 | .90 | .90 | .90 | .90 | .90 | .90 | .90 | .90 | .90 | .90 | .90 | .90 | .90 |
| 11 | $G_F/G_R$ | .35 | .38 | .42 | .45 | .50 | .55 | .60 | .65 | .72 | .78 | .85 | .93 | 1.02 | 1.11 | 1.22 | 1.33 | 1.46 | 1.59 |
| 12 | $G_{rms}$ Fus Norm | .03 | .05 | .08 | .11 | .25 | .54 | .70 | .99 | 1.36 | 1.12 | 1.15 | .92 | .59 | .50 | .44 | .43 | .33 | .30 |
| 13 | $G_L/G_R$ | .64 | .77 | .70 | .84 | .86 | .93 | 1.10 | 1.34 | 1.34 | 1.50 | 1.20 | 1.09 | .95 | .86 | .82 | .77 | .75 | .70 |
| 14 | $G_{rms}$ Fus Lat | .02 | .04 | .06 | .09 | .22 | .51 | .77 | 1.33 | 1.82 | 1.68 | 1.38 | 1.0 | .56 | .43 | .36 | .33 | .25 | .21 |
| 15 | $G_T/G_R$ | .62 | .60 | .56 | .55 | .55 | .51 | .59 | .61 | .57 | .56 | .54 | .58 | .47 | .45 | .46 | .44 | .43 | .48 |
| 16 | $G_{rms}$ Fus Tan | .02 | .03 | .04 | .06 | .14 | .28 | .41 | .60 | .78 | .63 | .62 | .53 | .28 | .23 | .20 | .19 | .14 | .14 |
| 17 | $G_{rms}$ Fus Worst | .03 | .05 | .08 | .11 | .25 | .54 | .77 | 1.33 | 1.82 | 1.68 | 1.38 | 1.0 | .59 | .50 | .44 | .43 | .33 | .30 |

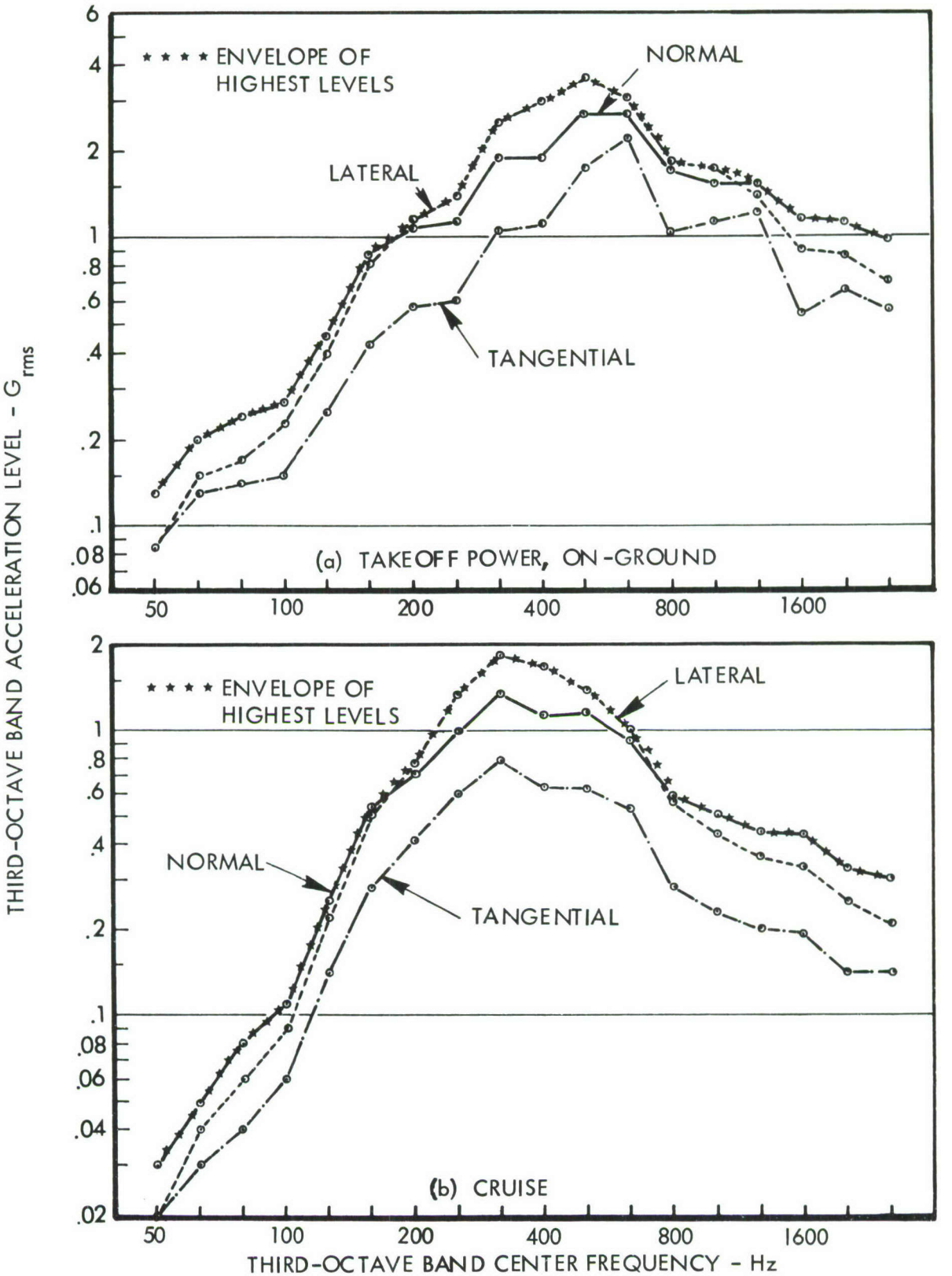


FIGURE 26. HYPOTHETICAL AIRCRAFT VIBRATION PREDICTION; FUSELAGE STRUCTURE

TABLE II — HYPOTHETICAL AIRCRAFT VIBRATION PREDICTION

WING - TAKEOFF

| | | THIRD-OCTAVE BAND CENTER FREQUENCY - Hz | | | | | | | | | | | | | | | | | |
|---|---|---|---|---|---|---|---|---|---|---|---|---|---|---|---|---|---|---|---|
| | | 50 | 63 | 80 | 100 | 125 | 160 | 200 | 250 | 315 | 400 | 500 | 630 | 800 | 1000 | 1250 | 1600 | 2000 | 2500 |
| 1 | Ref Box $G_{rms}$ | .38 | .54 | .61 | .71 | .82 | .76 | 1.1 | 1.6 | 1.7 | 1.9 | 2.0 | 2.4 | 3.2 | 2.2 | 1.5 | .90 | .73 | .52 |
| 2 | $C_3$ | 1.1 | 1.1 | 1.1 | 1.1 | 1.1 | 1.1 | 1.1 | 1.1 | 1.1 | 1.1 | 1.1 | 1.1 | 1.1 | 1.1 | 1.1 | 1.1 | 1.1 | 1.1 |
| 3 | Wing $G_{rms}$ Norm | .42 | .59 | .67 | .78 | .90 | .84 | 1.21 | 1.76 | 1.87 | 2.09 | 2.2 | 2.64 | 3.52 | 2.42 | 1.65 | .99 | .80 | .57 |
| 4 | $G_L/G_R$ | .65 | .78 | .71 | .85 | .86 | .95 | 1.15 | 1.48 | 1.56 | 1.95 | 1.45 | 1.15 | 1.06 | 1.11 | .91 | .79 | .77 | .71 |
| 5 | Wing $G_{rms}$ Lat | .27 | .46 | .48 | .66 | .78 | .79 | 1.39 | 2.6 | 2.92 | 4.08 | 3.19 | 3.04 | 3.73 | 2.69 | 1.5 | .78 | .62 | .41 |
| 6 | $G_T/G_R$ | .78 | .72 | .65 | .68 | .62 | .58 | .70 | .73 | .76 | .72 | .80 | .97 | .63 | .72 | .81 | .47 | .56 | .55 |
| 7 | Wing $G_{rms}$ Tan | .33 | .42 | .44 | .53 | .56 | .49 | .85 | 1.28 | 1.42 | 1.5 | 1.76 | 2.56 | 2.22 | 1.74 | 1.34 | .47 | .45 | .31 |
| 8 | Wing $G_{rms}$ Worst | .42 | .59 | .67 | .78 | .90 | .84 | 1.39 | 2.6 | 2.92 | 4.08 | 3.19 | 3.04 | 3.73 | 2.69 | 1.65 | .99 | .80 | .57 |

WING - CRUISE

| | | | | | | | | | | | | | | | | | | | |
|---|---|---|---|---|---|---|---|---|---|---|---|---|---|---|---|---|---|---|---|
| 9 | Ref Box $G_{rms}$ | .045 | .095 | .046 | .095 | .15 | .079 | .12 | .21 | .33 | .39 | .50 | .81 | 1.3 | 1.3 | .92 | .65 | .60 | .43 |
| 10 | $C_3$ | 1.1 | 1.1 | 1.1 | 1.1 | 1.1 | 1.1 | 1.1 | 1.1 | 1.1 | 1.1 | 1.1 | 1.1 | 1.1 | 1.1 | 1.1 | 1.1 | 1.1 | 1.1 |
| 11 | Wing $G_{rms}$ Norm | .05 | .10 | .05 | .10 | .17 | .09 | .13 | .23 | .36 | .43 | .55 | .89 | 1.43 | 1.43 | 1.01 | .71 | .66 | .47 |
| 12 | $G_L/G_R$ | .62 | .74 | .67 | .81 | .82 | .80 | .83 | .78 | 1.06 | 1.0 | 1.03 | 1.08 | .93 | .90 | .86 | .77 | .77 | .71 |
| 13 | Wing $G_{rms}$ Lat | .03 | .074 | .03 | .08 | .14 | .072 | .11 | .18 | .38 | .43 | .57 | .96 | 1.33 | 1.29 | .87 | .55 | .51 | .33 |
| 14 | $G_T/G_R$ | .39 | .41 | .36 | .27 | .32 | .29 | .28 | .26 | .26 | .37 | .40 | .46 | .46 | .50 | .59 | .46 | .53 | .54 |
| 15 | Wing $G_{rms}$ Tan | .02 | .04 | .02 | .027 | .05 | .03 | .04 | .06 | .09 | .16 | .22 | .41 | .66 | .71 | .60 | .33 | .35 | .25 |
| 16 | Wing $G_{rms}$ Worst | .05 | .10 | .05 | .10 | .17 | .09 | .13 | .23 | .38 | .43 | .57 | .96 | 1.43 | 1.43 | 1.01 | .71 | .66 | .47 |

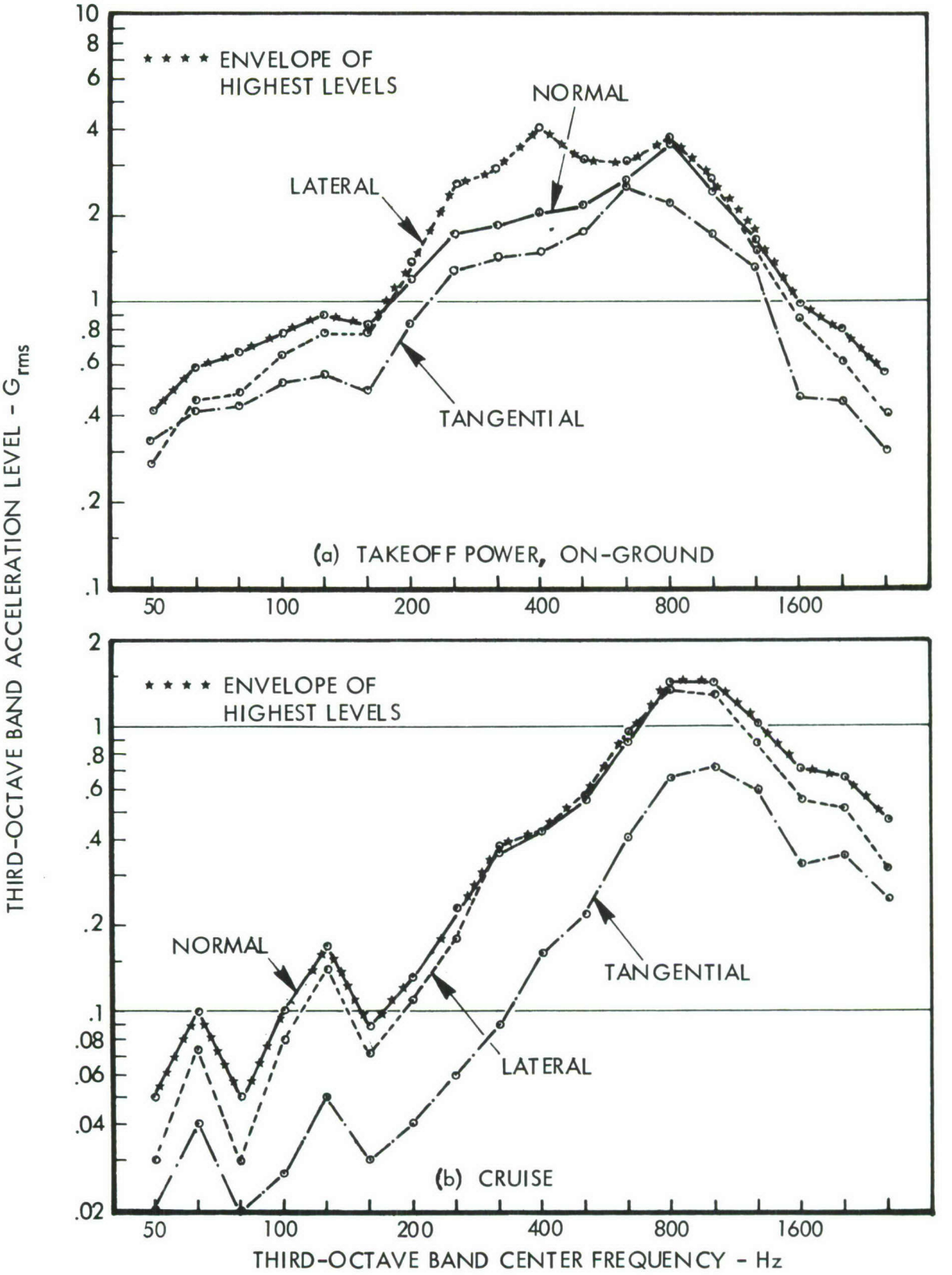


FIGURE 27. HYPOTHETICAL AIRCRAFT VIBRATION PREDICTION; WING STRUCTURE

## BIBLIOGRAPHY


- "Method for Predicting Environmental Vibration Levels in Jet Powered Vehicles," Noise Control, Mahaffey and Smith, July 1960.
- "Structural Vibration in Space Vehicles," WADD TR 61-62, Section III, Eldred, Roberts, and White, 1961.
- "Empirical Prediction of Space Vehicle Vibration," Shock, Vibration, and Associated Environments Bulleting No. 29, Part IV, Eldred, 1961.
- "New Approaches to Flight Vehicle Structural Vibration Analysis and Control," ASD-TDR-62-237, Heckl, Lyon, Maidanik, & Ungar, 1962.
- "Sound-Induced Vibrations of Cylindrical Vehicles," Journal, ASA, Franken, April, 1962.
- "Statistical Techniques for Predicting Localized Vibratory Environments of Rocket Vehicles," NASA TND-1836, Barrett, 1963.
- "A Technique for Predicting Localized Vibration Response in Rocket Vehicle Structure," Shock, Vibration, and Associated Environments Bulletin No. 33, Part II, Jewell, 1964.
- "Empirical Correlation of Excitation Environment and Structural Parameters with Flight Vehicle Vibration Response," AFFDL-TR-64-160, White, Bozich, Eldred, 1964.
- "Sound and Structural Vibration," NASA CR-160, Smith and Lyon, 1965.
- "Prediction of Flight Vibration Levels for the Scout Launch Vehicle," The Shock and Vibration Bulletin No. 36, Part 5, Bost, 1967.
- "Structural-Acoustic Response, Etc., of an Aircraft Fuselage, Etc.," AFFDL-TR-68-2, Cockburn and Jolly, 1968.
- "Statistical Analysis of Flight Vibration and Acoustic Data," AFFDL-TR-68-92, Piersol and Laan, 1970.

## BIBLIOGRAPHY - CONTINUED


- "Empirical Correlation of Flight Vehicle Vibration Response," The Shock and Vibration Bulletin No. 37, Part 7, Roberts, 1968.

- "Computer Programs for Prediction of Structural Vibrations Due to Fluctuating Pressure Environments," The Shock and Vibration Bulletin No. 40, Part 3, Lee and Swanson, 1969.

- "Assessment of Space Vehicle Aeroacoustic-Vibration Prediction, Etc.," NAS CR-1596, Himelblau, Fuller, and Scharton, 1970.

- "A Guide for Predicting the Vibrations of Fighter Aircraft in the Preliminary Design Stages," AFFDL-TR-71-63, Ungar, Madden, Lyon, and Bender, 1973.

- "Transonic Rocket-Sled Study of Fluctuating Surface-Pressures and Panel Responses," The Shock and Vibration Bulletin No. 42, Part 4, Ungar, Bandgren, and Erwin, 1972.

- "Summary of Random Vibration Prediction Procedures," NASA CR-1302, Barvoski, et al., 1969.

- "Structural Vibration Prediction," NASA Space Vehicle Design Criteria, NASA SP-8050, Anon, 1970.

- "An Assessment of Preliminary Design Methods for Predicting Vibration Due to Fluctuating Pressures," The Shock and Vibration Bulletin No. 43, Supplement 1, Marsh and Bingman, 1973.

UNCLASSIFIED

Security Classification

**DOCUMENT CONTROL DATA - R & D**

*(Security classification of title, body of abstract and indexing annotation must be entered when the overall report is classified)*

1. ORIGINATING ACTIVITY *(Corporate author)*

LOCKHEED-GEORGIA COMPANY
MARIETTA, GEORGIA 30063

2a. REPORT SECURITY CLASSIFICATION

UNCLASSIFIED

2b. GROUP

3. REPORT TITLE

A METHOD FOR PREDICTING ACOUSTICALLY INDUCED VIBRATION IN TRANSPORT AIRCRAFT

4. DESCRIPTIVE NOTES *(Type of report and inclusive dates)*

Final Report

5. AUTHOR(S) *(First name, middle initial, last name)*

Bartel, Harold W.
Schneider, Cecil W.

| 6. REPORT DATE | 7a. TOTAL NO. OF PAGES | 7b. NO. OF REFS |
|---|---|---|
| September 1974 | 44 | None |

| 8a. CONTRACT OR GRANT NO. | 9a. ORIGINATOR'S REPORT NUMBER(S) |
|---|---|
| F33615-73-C-3638 | |
| b. PROJECT NO. 1370 | LG74ER0121 |
| c. TASK NO. 137002 | 9b. OTHER REPORT NO(S) *(Any other numbers that may be assigned this report)* |
| d. | AFFDL-TR-74-74, Appendix I |

10. DISTRIBUTION STATEMENT

Approved for Public Release; Distribution Unlimited

| 11. SUPPLEMENTARY NOTES | 12. SPONSORING MILITARY ACTIVITY |
|---|---|
| | Air Force Flight Dynamics Laboratory, AFSC, Wright Patterson AFB, Ohio 45433 |

13. ABSTRACT

A method is set forth for predicting the acoustically induced structural vibration in transport category aircraft. Charts are presented which correlate third-octave random noise and vibration levels at various confidence levels, for the frequency range of 50 to 2500 Hertz. The prediction charts are based on measured data from modern transport aircraft and are presented for the normal direction, ground operation, and a reference structural mass and rigidity. Shell-type structure (fuselage, pods, fairings) and box-type structure (wing, horizontal/vertical stabilizer) are treated separately. Means are provided for predicting lateral and tangential vibration, vibration in pressurized cruise flight, and for correcting for changes in structural mass and rigidity. Application of the method to a hypothetical airplane design case is illustrated in an example.

14. KEY WORDS:

Acoustically Induced Vibration
Aircraft Vibration
Dynamic Response
Structural Vibration
Vibration Prediction

DD FORM 1 NOV 65 1473

UNCLASSIFIED

Security Classification

☆U.S.Government Printing Office: 1974 — 657-017/339